Title: NANO LIPID CARRIER BASED TARGETED DUAL DRUG DELIVEY OF 5-FLUOROURACIL AND CANNABIDIOL FOR TREATMENT OF SKIN CANCER.

Introduction:

The skin cancer is known as one of the deadliest diseases and a threat to public health. The prevalence of skin cancer is expanding steadily through distinct geographical regions (Australia and the United States) based on exposure to hazardous chemicals and ultraviolet radiation [1]. For this, a range of various chemotherapies have been established for the treatment of skin cancer; specifically, certain chemotherapeutics such as 5-Fluorouracil, Vismodegib, and Imiquimod have been proved to be effective candidates for the treatment of skin cancer [2]. The occurrence of non-melanoma skin cancer involves multiple molecular events and alterations in pathways which are pro-oncogenic factors to initiate this deadliest skin disease [1]. Initially, the inflammation and constant hyperplasia in the epidermal layers lead to the development of the initial stage of cancer cells [3]. Conventional chemotherapies are imperfect due to unfocused targeting of drug. The deep-seated location of tumor within the complex anatomy is also responsible for lower efficacy of drugs [4] .

The cancers cells develop protective mechanism against conventional therapies thus to tackle that problem targeting cancerous cells by multiple bio- chemical pathways is an alternate way to inhibit chemo resistance. It is well reported that nanoparticles with multiple payloads including anti-cancer drug and chemosensitizers were more efficient in targeting as well as killing of cancerous cells. The combination drug therapy or multi-targeted payload in a single nanomedicine (MTPNs) has impressively evolved in recent years. MTPNs are more efficacious and are less prone to drug resistance compared to conventional chemotherapy. MTPNs show better therapeutic effect as they target the cancer by multiple sites of action [5]–[8]. Cannabidiol is one of the hot molecules of decade and its various preclinical and clinical studies exhibited the potential of cannabis against various diseases, including cancer and related pain. Besides the well- known psychotropic effects of cannabis upon the use at high doses, literature has also shown the importance of cannabis and its constituents in minimizing the lethality of cancer in the preclinical models [9].

The problems of the low uptake due to the barrier function of the stratum corneum is a major obstacle with the topical delivery of the combination has been studied and investigated for the transport of the therapeutic substance to the skin, the advantages of NLCs are as follows: a disordered crystal structure, which can help prevent leakage of the drug load and providing higher drug payload [10]. NLC have many features that are advantageous for the skin targeting. They are composed of physiological and completely biodegradable solid lipid and

liquid lipids and exhibiting low toxicity. Their small size ensures a close contact with the skin and increase the amount of the drug penetrated into skin [11]. They enhance the drug permeation into the skin, increase skin hydration, enhance chemical stability of drug, minimize skin irritation and thus improve benefit/risk ratio. They are reported to enhance the bioavailability of topically applied drugs, increasing skin penetration. Their small particle size ensures close contact to the SC and thus, the amount of encapsulated drug reaching the site of action will be increased. topical application of aqueous NLC dispersions creates a mono-layered lipid film via gel onto the skin, which prevents trans epidermal water loss, thus increasing skin's moisture and hydration. Besides these potential advantages of the NLC in topical drug delivery, NLC enhance sun blocking[12].

Considering all scientific evidences, we hypothesize a novel dual-drug (CBD and 5-FU) loaded lipid-based nanocarriers for the superior chemotherapy. Notably, these developed nanocarriers incorporated in the gel to ease the application of drugs via topical route. This combination (CBD and 5-FU) did not improve the pharmaceutical attributes only, but, improved the overall bioavailability and reduced the required dose of CBD and 5-FU to regress the tumor progression. The combination of 5-FU and CBD which is encapsulated in nanostructured lipid carrier, later, incorporated in the gel to target the skin layer is novel. Overall, this investigation demonstrated the efficacy of these two drugs in skin cancer by improving the sensitivity of 5-FU and CBD for the effective therapy. Firstly, 5-FU and CBD loaded nanocarrier gel-based formulation was prepared and its diposition pattern in different layers of skin was observed by confocal microscopy. Then, safety of the formulation was observed by skin irritation studies followed by skin retention studies were carried by gamma scintigraphic analysis. Further, therapeutic efficacy of prepared formulation was established by *In-ovo* analysis. Later, *In-ovo* analysis was validated by *In-vivo* tumor remission studies followed by biochemical estimation. Thus, at the end of the study overall aim to develop novel gel for non-melanoma skin cancer with better therapeutic efficacy was achieved.

the complex anatomy is also responsible for lower efficacy of drugs [4]. Then, safety of the formulation was observed by skin irritation studies followed by skin retention studies were carried by gamma scintigraphic analysis. Further, therapeutic efficacy of prepared formulation was established by *In-ovo* analysis. Later, *In-ovo* analysis was validated by *In-vivo* tumor remission studies followed by biochemical estimation. Thus, at the end of the study overall aim to develop novel gel for non-melanoma skin cancer with better therapeutic efficacy was achieved.

1. Methods:

1.1 HPLC Instrument and Chromatographic Conditions

HPLC was carried out on Waters® e2695, equipped with a Quaternary pump with Photodiode array Waters® 2998 detector and EMPOWER 3 software. Hypersil™ C18 reverse phase column 250 mm × 4.6 mm, 5µm was used. Analysis was carried out by PDA detector at wavelength 267 nm, 220 nm and 237 nm for 5-FU, CBD and FU-CBD mixture, respectively [20, 23, 24]. Linear gradient elution flow was 85% to 100% of methanol over 2.5 minutes, which then held at 100% methanol for 2 minutes at a flow rate of 0.75 ml/min and at a controlled column temperature of 25°C. The injection volume was 10 µl while analysis time was set to 4 minutes.

1.2. Risk Assessment Study

A risk assessment study was performed to identify the few vital variables which may influence the method performance. For identifying the high-risk factors, a formal risk estimation matrix was constructed by assigning low, medium and high-risk scores to each of the method variables. Only the medium to high-risk parameters were identified and subjected to risk minimization by adopting a suitable risk mitigation strategy.

1.3. Preparation of Standard and Working Solutions

Standard solutions of 1000 µ g/ml 5-FU and CBD were separately prepared using methanol and named as A1 and A2 for 5-FU and CBD, respectively. From standard solutions, stock solutions were prepared to have a concentration of 100µg/ml and named as S1 and S2 for 5-FU and CBD, respectively. Solutions with a concentration of 10, 20, 40, 80, 100 µg/ml were prepared from stock solutions S1 and S2 for 5-FU and CBD, respectively, using methanol as the diluent.

Similarly, for FU-CBD combination, samples with concentrations of 10, 20, 40, 80, 100 µg/ml of both the drugs were prepared in methanol. Further, QC (quality control) samples, such as LQC (lower quality control), MQC (middle quality control) and HQC (higher quality control) samples having concentrations 10, 15 and 20 µg/ml, respectively, were prepared for both drug samples 5-FU and CBD. All prepared samples were filtered through a syringe filter having a pore size of 0.22 µm (millifilter, Milford, USA) [25, 26].

1.4. Preparation of Standard Plasma and Working Solution

A stock solution with a concentration of 100 µg/ml of 5- FU and CBD was separately prepared in methanol and named S1P and S2P for 5-FU and CBD, respectively. From stock solution, S1P and S2P with sufficient dilution from methanol 2 ml at following concentration of 10, 20, 40, 80, 100 µg/ml were prepared; 100 µl of plasma was added to each prepared

concentration and then samples were vortexed for 15 minutes. After vortexing, samples were centrifuged at 5000 rpm at a controlled temperature of 24 • } 2°C for 15 minutes; then, the supernatant was carefully separated, filtered through a syringe filter having a pore size of 0.22 μm, and analyzed at 220, 267 and 237 nm, respectively [27].

2. VALIDATION

Validation of the method was performed according to ICH guidelines, in terms of system suitability test, specificity, linearity, ruggedness, limit of detection and limit of quantification [28].

2.1. System Suitability Test

It is an important tool for liquid chromatographic procedures that helps to validate the testing procedure for its application and guarantees reproducible results. The suitability test was done at 20 μg/ml of 5-FU and CBD MQC level via injection of six replicates; the results were analyzed through peak area and RT of both the analytes at 237 nm. As per the criteria set by US-FDA for this test relative standard deviation, %RSD of peak area and retention time should be less than 2% [27].

2.2. Specificity

The main characteristic feature of HPLC is specificity which is defined as the ability to separate the analyte from the mixture in the analytical system. Evaluation of specificity was done by comparing individual solution chromatograms with a blank solution and their mixture. 5-FU and CBD were not added in the blank solution; the rest of the composition and method of preparation were the same as those of the sample solution.

2.3. Linearity

Five mixed standard solutions with different concentrations were prepared for determination of linearity ranging between 10-100 μg/ml, in the concentration of 10, 20, 40, 80 and 100 μg/ml, respectively. Calibration curves of 5-FU, CBD and FU-CBD were prepared separately by plotting concentration on the X-axis and peak area on the Y-axis, and the regression equation was derived from it. The response ratio (response factor) was also calculated through the division of peak area with concentration.

2.4. Ruggedness

The ability to reproduce the result under various circumstances, such as different analysts or different instruments, is called ruggedness. For our study, the ruggedness was tested by using three different samples having a theoretical concentration of 10, 20 and 30 μg/ml, analyzed by two different analysts on identical HPLC instruments in the same and different labs.

Percentage recovery was calculated for both the analytes; results noted by two different analysts were compared for the ruggedness [29].

2.5. Sensitivity

Estimation of sensitivity was done on the basis of LOQ (limit of quantification) and LOD (limit of detection). The signal-to-noise ratio calculated in the case of LOD concentration is approximately 3:1, and in the case of LOQ concentration, the ratio is 10:1 with a percentage RSD of less than 10% (n = 3). Following equations (1 and 2) were used to determine LOD and LOQ of the analytes, where σ is the standard deviation of the response (peak area) and s is the slope obtained in the calibration curve.

3. ANALYTICAL METHOD FOR PHARMACEUTICAL NANOFORMULATIONS

3.1. Preparation of FU-CBD Liposome

Film formation technique was employed to formulate 5- FU and CBD-loaded liposomes (FU-CBD-L). Cholesterol and Phospholipon 90 were used in ratios 40:60, respectively.

In methanol:chloroform ratio (2:1), weighed amount of cholesterol, lipids, 5-FU and CBD were dissolved. Thereafter, thin lipid film was prepared by evaporating organic solvents using a round bottom flask on a rotary evaporator (Buchi, Switzerland). Prepared FU-CBD lipidic film on round bottom flask was hydrated using 5 ml milli-Q water at 100 rpm for 60 minutes to obtain liposome dispersion of FU-CBD. Obtained dispersion was then ultrasonicated under an ultraprobe sonicator for 30 seconds. Prepared FU-CBD-L dispersion was centrifuged at 4°C at 15000 rpm for 30 minutes; then the supernatant was separated and obtained FU-CBD-L pellet was redispersed in milli-Q water, and then redispersed FUCBD- L were analyzed for percentage drug encapsulation [30].

3.2. Preparation of FU-CBD SLN

FU-CBD SLN were prepared using melt emulsification technique by using Gelucire 50/13 as solid lipid. The lipid phase was prepared by melting an accurately weighed amount of Gelucire 50/13 at 60-70°C, then Transcutol P was added to it, which was followed by adding a prerequisite amount of 5-FU and CBD. The aqueous phase was prepared by dispersing Poloxamer 407 in milli-Q water and the temperature was raised to 60-70°C at this point; the lipidic phase was added to the aqueous phase with continuous stirring of 600 rpm for 30 minutes that led to the formation of primary emulsion. Primary emulsion was sonicated by ultra-probe sonicator for 30 seconds; thus, obtained dispersion was kept on the cool surface, which led to the formation of FU-CBD SLN. The obtained FU-CBD SLN dispersion was then centrifuged for 30 minutes with a controlled temperature of 4°C at 15000 rpm to

separate prepared FU-CBD SLN. The obtained supernatant was discarded, whereas obtained pellet was redispersed in milli-Q water and percentage entrapment was calculated for 5-FU and CBD [31, 32].

3.3. Preparation of FU-CBD NLC

FU-CBD NLC were prepared using melt emulsification technique by using Gelucire 50/13 as solid lipid and coconut oil as liquid lipid. The lipid phase was prepared by melting accurately weighed amount of Gelucire 50/13 and coconut oil at 60-70°C; then, Transcutol P was added to it, which was followed by the addition of prerequisite amount of 5-FU and CBD. The aqueous phase was prepared by dispersing Tween 80 and Poloxamer 407 in milli-Q water and the temperature was raised to 60-70°C; at this point, lipidic phase was added to the aqueous phase with continuous stirring of 600 rpm for 30 minutes that led to the formation of primary emulsion. Primary emulsion was sonicated by ultra-probe sonicator for 30 seconds; thus, obtained dispersion was kept on the cool surface, which led to the formation of FU-CBD NLC. The obtained FU-CBD NLC dispersion was then centrifuged for 30 minutes at a controlled temperature of 4°C at 15000 rpm to separate prepared FU-CBD NLC. The obtained supernatant was disposed off, whereas obtained pellet was redispersed in milli-Q water, and percent entrapment was calculated for 5-FU and CBD [13].

4. In-silico study

All the Computational studies presented such as molecular docking, MM-GBSA, and ADME analysis were performed on Schrodinger Maestro version 10.5 on windows 10, hp desktop computer with 64-bit operating system, intel core 7th generation processor, 4GB Intel graphics card, 16GB RAM. Firstly, Ligand preparation was initiated by generating the structure of Cannabidiol and 5- Fluorouracil in chem draw tool version 16.0 in cdx format, further both the ligands were converted to mol-sd file format and then subjected to LigPrep module of Maestro, in which Ligands were prepared and all energies were minimized. At pH 7.0 ± 2.0, the all-possible ionization states were generated and minimized. Then, Protein preparation and receptor grid generation of the crystal structure of p38 MAP kinase (PDB ID: 2GTM) was retrieved from RCSB Protein Data Bank. Imported Protein was further pre-processed, optimized, and minimized using the protein preparation wizard panel. Ligand bound with the protein is selected for receptor grid generation by selecting amino acid residues method reported by Haider et al. using receptor grid generation panel of Glide version 6.9 [21]. Further, Glide Ligand Docking was performed using the receptor grid module and the ligand molecules which were previously prepared, where the glide docking of the proposed molecule was carried out. The favorable interactions between ligand molecules

and the receptor were scored using the Glide ligand docking system (Dock Score). All the docking calculations were done in extra-precision (XP) mode; OPLS-2005 force fields were used.

5. Compatibility studies

For the determination of compatibility of 5-FU and CBD and to observe any possible interaction between both compounds FT-IR spectroscopy (Fourier transform infrared spectroscopy) was employed. Briefly, 5-FU and CBD were mixed in a 1:1 ratio and the mixture was kept at a temperature of 25 ± 2 °C and relative humidity (%RH) of 60 ± 5% for 28 days. FT-IR analysis of 5FU, CBD, and the mixture was performed on day 1 and day 28 [12].

6. Excipient's screening study

6.1 Screening of Lipids

Excipient's selection is a major part of formulation development. Thus, for the preparation of FU-CBD NLCs solid lipid selection was performed. Solubility of 5-FU in various solid lipids (Geleol, compritol® 888 ATO, precirol® ATO 5, Gelucire® 50/13, and Gelucire® 44/14 was evaluated by saturated solubility method. 5-FU was added in increments to molten solid lipids (previously heated 5-10˚ C to their respective melting point) till saturation level was achieved by visual observation. After completion of the study, the amount of 5-FU solubilized in each lipid was calculated and the selection of solid lipid was done on the basis of lipid which solubilizes the maximum. After the selection of solid lipids, various liquid lipids were screened based on their respective solubility for 5-FU. In this excess amount of 5-FU was added in different oils such as capryol® 90, Labrasol®, Campul®, Castor oil, Olive Oil, Oleic Acid, and coconut oil. Preliminary mixing of drug and oil was performed using a vortex mixer for the time interval of 10 minutes followed by continuous stirring at room temperature for 72 hours in a mechanical shaker (Lab Therm, Kuhenr Switzerland). After that, samples were subjected for centrifugation for 30 minutes at 5000 rpm at room temperature (Remi Pvt Ltd, Maharashtra, India). Then, the supernatant was separated from resultant mixture obtained after centrifugation and dissolved in methanol and the solubility of 5-FU in respective oils was determined using a UV spectrophotometer (Shimadzu, Japan, Model no. UV-1601) at the wavelength of 267 nm respectively.

6.2 Screening of Binary mixture ratio

The selected solid-lipid and liquid-lipid ratios were optimized for nanoformulation development. Screening of binary mixture was performed by visual and DSC analysis. The binary mixture containing Solid-lipid and Liquid-lipid (SL: LL) was prepared in 10:0, 9:1,

8:2, 7:3, and 6:4, 5:5 ratios. Then, samples were kept at 70°C in the water bath for 1 hour with continuous agitation. After 1 hour, the samples were kept for 24 hours at room temperature and firstly analyzed visually against the light. Binary mixtures (BM) which show cracking or phase separation were rejected and BM which was uniform were selected for DSC thermal analysis. All selected BM samples were scanned for change in any thermal event by taking pure solid lipid as standard. Briefly, the thermal analysis was performed using Differential Scanning Calorimetry (DSC) (Perkin Elmer Pyres, USA) with constant nitrogen gas flow and heating rate of 10°C per minute for a temperature range of 30-100°C. then the crystallinity index (CI) of each BM was calculated using the following equation 1.

$$\mathrm{CI} = \left(\frac{\Delta \mathrm{HBM}}{\Delta \mathrm{HSL}}\right) 100 \quad \text{..... Equation 1}$$

Where, ΔHBM represents the enthalpy of BM, while ΔHSL represents the enthalpy of pure solid lipid [24].

6.3 Screening and selection of surfactant and co-surfactant

The emulsification potential of several surfactants including Poloxamer 407 (Pluronic F-27), Cremophor EL, Tween 20, Tween 80, Transcutol P, and Cremophor RH40) was analyzed to emulsify the selected binary mixture. The method defined by Babar et al., 2018 was implemented. 100 mg of selected BM was dissolved in 3 mL methylene chloride then 10 mL of 5% surfactant solution was added and formed resulting mixture were kept over a magnetic stirrer for two hours at a controlled temperature of 40°C to remove methylene chloride. After the removal of methylene chloride. 1mL, the mixture was subjected to dilution with 10 mL of water which was analyzed at a wavelength of 510 nm for percentage transmittance using a UV spectrophotometer at room temperature [16].

6.4 Optimization of surfactant and co-surfactant concentration.

The ratio of the mixture of surfactant and co-surfactant (Smix) was optimized for preparing a stable formulation. Surfactant and co-surfactant were previously mixed in the mass ratio of 1:1, 2:1, 3:1, 4:1, and 5 :1 then, 100 mg of the binary mixture was added to each 1% aqueous solution of Smix with continuous stirring. After that, each solution was analyzed for percentage transmittance analyzed at the wavelength of 510 nm using a UV spectrophotometer at room temperature. The Smix ratio with the best emulsification value was selected for formulation development.

7. Formulation development and optimization

Formulation development was prepared using the spontaneous emulsification method. Briefly, the lipidic mixture was initially developed by adding 1% CBD in a melted 2% binary mixture. Then, aqueous phase was prepared by adding 1% of Smix to double distilled water. Primarily, 1% of 5-FU was added in 100µL of aqueous phase and this solution was then added to the lipidic phase dropwise with continuous stirring keeping the temperature at 70°C at 800 rpm over a magnetic stirrer (Tarsons, India) for 5 minutes to form primary emulsion. Next, the lipidic mixture was added dropwise to the aqueous phase under constant stirring at 800 rpm to obtain the NLCs, which is then stirred for next 30 minutes to stabilize the developed FU-CBD NLCs. Then, The central composite rotatable design (CCRD) was employed for optimization of FU-CBD NLCs formulation using Design Expert Software 11.1.1.0 (Stat-Ease Inc. Minneapolis). Firstly, Binary mixture concentration (%w/w), and Smix concentration(%w/w) were selected as independent variables with a range of 1-3% w/w and 0.5 - 2% respectively for optimization and their low and high limits were shown in Table 1. Particle size with in-range constraint, polydispersity index minimum, and entrapment efficiency of 5-FU and CBD with maximum constraint were selected as dependent variables for optimization studies.

Table 1 Enlists the Independent variables and dependent variable for the optimization of FU-CBD-NLCs by central composite rotatable design by DoE.

Factor	**Level Used**	
1. Independent Factor	**Low**	**High**
X_1 = Binary mixture concentration (% w/w)	1	3
X_2 = Smix concentration	0.5	2
2. Dependent Factor	**Constraint**	
Y_1 = Particle size (nm)	In range 200-250 nm	
Y_2 = PDI	Minimum	
Y_3 = entrapment efficiency 5-FU	Maximum	
Y_4 = Entrapment efficiency CBD	Maximum	

8. Characterization of developed formulation

8.1 Mean Particle size, zeta potential, and morphological examination

Prepared FU-CBD NLCs were characterized with respect to particle size (hydrodynamic diameter), surface charge (Zeta potential) and PDI (polydispersity index) analysis which was

conducted using photon correlation spectroscopy (PCS) by Particle Sizing Systems, Malvern nano ZS, Inc. UK). Prepared FU-CBD NLCs were diluted with Milli-Q water and loaded in sample inlet in the disposable cuvette for particle size and PDI analysis. For surface charge zeta potential cuvette was used for analysis. Each sample was analyzed in triplicate [27] . Surface morphology and particle shape of formulated FU-CBD NLCs were analyzed by Scanning Electron microscope (SEM) Leo Electron Microscopy Ltd.UK. Briefly, FU-CBD NLCs were diluted using Milli-Q water and placed on a copper sputter which was further coated with gold-palladium for surface charge minimization coated copper stub was placed in the sample inlet, and analysis was performed. After SEM analysis, Transmission Electron Microscopy (TEM) analysis of FU-CBD NLCs was performed using Transmission Electron Microscopy (TEM), Tecnai G2 S-twin, Netherland. TEM analysis was performed at the scale of 200 nm at 120 KV which have high resolution and point-to-point observation capability. A drop of diluted FU-CBD NLCs was placed on copper grids and samples were dried at room temperature. Dried sample-loaded copper grids were then placed in the sample port of TEM and images were captured. Captured images were analyzed using Keen View FM and Olympus Soft Imaging Viewer. Percent entrapment efficiency (EE) was determined by the indirect method described in [19]. The unentrapped concentration of 5-FU and CBD were determined in the aqueous phase of prepared FU-CBD NLCs dispersion. briefly, 5 mL of FU-CBD-NLCs dispersion was subjected to centrifugation at 14000 RPM for 20 mins at 4˚C. Furthermore, the supernatant of resultant FU-CBD NLCs dispersion after centrifugation was collected and free drug present in supernatant layer was determined at a wavelength of 260 nm and 220 nm for 5-FU and CBD respectively using UV-spectrophotometer (Shimadzu1800, Japan. Then, by using equations 2 (EE) was determined [7].

$$(\%EE)\ \text{Percent Entrapment efficiency} = \frac{\text{Initial Drug (mg)} - \text{Free Drug(mg)}}{\text{Initial Drug (mg)}} \times 100 \quad \text{Equation 2}$$

Where,

'Initial drug' is the weight amount of drug used to prepare FU-CBD-NLCs

'Free drug' is amount of drug present in supernatant layer

All the experiments were performed in triplicate for precise readings [32].

8.2 Differential Scanning Calorimetry analysis

Investigation of physical state, melting point, and any interaction among FU, CBD, and excipients used in the formulation of FU-CBD-NLCs were analyzed using DSC. Briefly,

DSC analysis of 5-FU, CBD, and lyophilized FU-CBD-NLCs. The formulation was lyophilized using a labconco Lyophilizer operated at a temperature of -50˚C with −0.01 MPa pressure for 72 hours which results in the formation of lyophilized FU-CBD-NLCs. After that, samples were analyzed for thermal property with a constant heating rate of 5˚C/min and constant nitrogen gas flow over the temperature range of 30˚C to 300˚C.

8.3 X-ray diffraction analysis (XRD)

To confirm the structural property of the pure drug and prepared formulation FU-CBD-NLCs XRD (X-Ray diffraction) patterns were determined using PW 1830, Philips equipped with an XRD commander program to investigate the crystalline peak of the sample which results in ensuring the physical state of the sample. Briefly, pure 5-FU, CBD, binary mixture, and Lyophilized powder of FU-CBD-NLCs were taken to the cell and then scanned at the range of 0 to 100 of 2-Theta at 35 KV AND 30 Ma using Lynx Eye detector [21].

9. In-vitro Cell line studies

9.1 MTT assay and combination index analysis

The human epidermoid carcinoma cell line (A431) was procured from National Centre for Cell Sciences (NCCS), Pune, India. Procured cell line was cultured using DMEM (Dulbecco's modified eagle medium) with additional supplementation of 1% and 10% v/v of antibiotic antimycotic solution and heat-inactivated FBS (Fetal Bovine Serum) respectively in T-75 flasks which were further stored at 37 °C under 5% CO_2 atmosphere.

In vitro toxicity of 5-FU, CBD and FU-CBD were evaluated using MTT (3-(4, 5-dimethylthiazol-2-yl)-2, 5-diphenyltetrazolium bromide) assay against A431 cells. A431 cells were plated in a 96-well plate for 24 h before treatment with 5-FU, FU-CBD, and FU-CBD-NLCs, in the appropriate concentration range. Briefly, the seeding of 4×10^4 Cells per well of 96 well plates was done. Then, cells were treated in the range of 0-30 µM of 5-FU, and 0-500 µM of CBD for 24 and 48 hours. After treatment cells were subjected to washing with PBS (phosphate buffer saline) of pH 7.4 followed by incubation of medium with MTT (5 mg/mL) for 4 hours at 37 °C leading to the formation of formazan crystals following dissolution in DMSO (200 µL). Then the optical density of the obtained solution was observed at 570nm using the iMark Microplate Reader (BioRad, USA). The percent viability was determined and IC_{50} of 5-FU and CBD was calculated.

9.2 Combination index analysis of 5-FU and CBD

To observe the combinatorial effect of 5-FU and CBD on skin cancer cells (A431) combination index analyses were performed. Briefly, various soluble combinations of both

drugs 5-FU and CBD were analyzed and the combined effect was calculated using the equation 3 mentioned in Zafar et al.

$$CI = \frac{a}{A} + \frac{b}{B}$$ ……. Equation 3

Where,

a and b are the concentration of 5-FU and CBD respectively in a combination system at their IC_{50}, separately and A and B are the IC_{50} of 5-FU and CBD when analyzed alone. The calculated CI values >1, 1, and <1 indicate combination antagonistic, additive, and synergistic effects of the combinatorial drug system respectively [22]. After selection of combinatorial dose IC_{50} of it was calculated in triplicate.

9.3 Assessment of cytotoxicity of prepared formulation

In vitro toxicity of combinatorial dose of 5-FU and CBD mixed in (1:9) and prepared FU-CBD-NLCs (having 5-FU and CBD in 1:9) was evaluated using MTT (3-(4, 5-dimethylthiazol-2-yl)-2, 5-diphenyltetrazolium bromide) assay against A431 cells. A431 cells were plated in a 96-well plate for 24 h before treatment with FU-CBD and FU-CBD-NLCs, in the appropriate concentration range. Briefly, the seeding of 4×10^4 Cells per well of 96 well plates was done. Then, cells were treated in a range of 0-500 µM of FU-CBD mixture and prepared FU-CBD-NLCs for 24 and 48 hours. After treatment cells were subjected for washing with PBS (phosphate buffer saline) of pH 7.4 followed by incubation of medium with MTT (5 mg/mL) at 37 °C for 4 hours leading to the formation of formazan crystals which were further subjected to dissolution in DMSO (200 µL) of DMSO. Then the optical density of the obtained solution was observed at 570nm using the iMark Microplate Reader (BioRad, USA). The percent viability was determined and IC_{50} of 5-FU, CBD mixture as well as prepared FU-CBD-NLCs was calculated in triplicates.

9.4 In vitro wound-healing assay

The wound healing study was done in accordance with the previously published method on A431 cells. The cells of density 1 × 105 cells/well were cultured in 12 well plates and were allowed for 24 and 36 hours. Scratch was made using a P10 Pipette tip, followed by treatment of cells with NS, FU, and FU-CBD-NLCs considering the IC_{50} value. The migration of cells across the wound was captured using a phase-contrast microscope at 0h, 24h, and 36h [12].

9.5 Nuclear morphology Assessment (DAPI staining Test)

DAPI (4′,6′- diamidino-2-phenylindole) staining has a high DNA affinity, Thus, it is commonly used for measuring the cell apoptosis, sorting cells based on DNA content, and in high-content imaging analysis as a nuclear segmentation tool. To determine the nuclear

morphology of A431 cells and the effect of 5-FU treated and FU-CBD-NLCs cell DAPI staining was employed. The experiment was conducted in 6 well plates and each well were seeded with 1.5×10^5 cells of A431 cells with DMEM medium. After 24 hours, treatment was given with calculated IC_{50} values of 5FU and FU-CBD-NLCs and kept for 48 hours. After the treatment for 48 hours, cells were separated and washed three times with phosphate buffer having pH 7.4, and obtained cells were fixed with the help of 4% of Paraformaldehyde (PFA). Then, fixed cells were washed with phosphate buffer for three times having pH 7.4 followed by the addition of 0.2% Triton X-100 to make cell membranes more permeabilize. After that, obtained permeable cells were subjected to incubation in 1 μg/mL of DAPI staining solution for 5 minutes, and then cells were permanently mounted and observed under a fluorescence microscope (Nikon Eclipse 80i) at emission wavelength of 486-nm and the excitation wavelength of 350 nm.

9.6 Cell Cycle Analysis

By the principle of flow cytometry, the cell cycle was evaluated using Propidium Iodide staining on a flow cytometer (BD Biosciences). The seeding of cells in 6-well plates was done and after 24 hr of the cell, attachment cells were treated with IC_{50} value 5-FU and FU-CBD-NLCs for 24 h. Washing of cells with PBS was done after 24 and were subject to trypsinization. Cells pellet was collected and fixed with chilled 70% ethanol and stored at -20^{o}C overnight. Fixed cells were centrifuged and the pellet was re-suspended in 50 μg/mL PI and 100 μg/mL RNase-A staining solution. In G1, G2/M and S phases, the Different percentages of cells in the cell cycle were observed by flow cytometry (BD FACSAria III; BD Biosciences) with BD FACSDiva 8.0.2 software (BD Biosciences) [23].

10. FU-CBD NLCs gel formulation

The Carbopol 934 (1% w/v) was used as a gelling agent and was used for conversion of Optimized FU-CBD NLCs into FU-CBD NLCs gel. Carbopol 934 poses several unique properties including a sparkling appearance, good cohesive properties, and have easy wash-off nature. Briefly, 1% Carbopol 934 was accurately weighed and added to water with continuous stirring at stir rate of 1200 RPM on a magnetic stirrer (Remi Motors Ltd., India). Carbopol 934 was kept on stirring overnight to swell up, further, swollen Carbopol base was neutralized by 0.05% w/w of triethanolamine to form a gel. Then optimized FU-CBD formulation was added slowly to the formed gel with vigorous stirring. Finally, a preservative (0.01% benzalkonium chloride) was added to form an FU-CBD gel[24].

11. Evaluation of FU-CBD NLCs Gel Formulation

Evaluation of FU-CBD NLCs gel (FU-CBD-G) Formulation was firstly examined on the following parameters Homogeneity, Physical Examination, and pH. Further evaluation of FU-CBD-G was evaluated based on Extrudability, Spreadability, and Texture profile analysis characteristics of FU-CBD-G.

11.1 Homogeneity, Physical Examination, and pH

Firstly, a Physical Examination was conducted and prepared FU-CBD-G was visually inspected for any separation, consistency and Homogeneity. The homogeneity test of FU-CBD-G formulation was conducted by pouring prepared gel into the container and then prepared gel was visually observed for homogeneity. Later, pH evaluation of FU-CBD-G was done by pH meter (Microprocessor pH system, India). All experiments were performed in triplicate at 25 ± 1ºC. [39].

11.2 Spreadability and Extrudability

The Spreadability of FU-CBD-G was determined by its drag and slip properties. Briefly, 1g of FU-CBD-G was poured between two slides i.e., the lower and upper slide. A balance hook was attached to the upper slide while the Lower slide was fixed at the bottom side. The shift of the upper slide from its position and the time taken was recorded when known weights were added to the balance hook [25]. The measurement was taken in triplicate and Spreadability was determined using equation 4.

$$S = \frac{m \times L}{t} \quad \text{……Equation 4}$$

Where S, L, t, and m represent Spreadability (g/sec.), fixed distance, time (s), and weight respectively.

An extrudability test of prepared FU-CBD-G was performed to observe the extrudability property of prepared FU-CBD-G from the tube. In collapsible tube was FU-CBD-G filled and to avoid any leakage filled tube was sealed. The pressure was applied on the tube for 10 seconds, pressure at which 0.5 cm ribbon of prepared FU-CBD-G was extruded from the tube was the point extrudability was calculated using equation 5.

$$E = W/A \quad \text{……Equation 5}$$

Where, E, A, and W stand for extrudability, Area and applied weight to extrude gel from tube respectively.

11.3 Rheological Studies characterization of FU-CBD gel

The viscosity and viscoelastic behavior of FU-CBD-NLCs gel was determined by using MCR 101 Rheometer (Anton Paar, Germany) attached with water bath having thermostatically controlled circulating system, using cone and plate (CP-50-1) and plate & plate geometry (PP-2-5) operated by Rheoplus software. Experiments were performed at the temperature of 25 ±0.5˚C in triplicates. Initially, the flow behavior of the FU-CBD-NLCs gel was determined by a flow curve test containing viscosity (Pa. s) and shear stress (τ), which were measured at different shear rates ranging from 0.1 to 100 s−1 [28]. Furthermore, the amplitude sweep test was employed for determining viscoelastic behavior. Further, Linear viscoelastic region (LVR) was determined by measuring G" (loss modulus) and G' (storage modulus) by varying shear stress (Pa) from 0.05 to 100 Pa while keeping the frequency of 1 Hz constant. Afterwards, an oscillation frequency sweep test was conducted at constant strain and varying frequencies to observe the behavior of prepared FU-CBD-NLCs gel, in which, G" (loss modulus), G' (storage modulus) and complex viscosity (η) were measured by keeping 1% constant strain amplitude in the linear viscoelastic region and the frequency (Hz) ranging from 100 to 0.01 Hz [44].

11.4 Texture profile analysis of FU-CBD-G

Parameters of gel such as the force of adhesion, gel strength, hardness (HA), cohesiveness (CO), springiness (SP), and firmness of prepared FU-CBD-G were analyzed using TA. XT plus Texture Analyzer (Stable Micro System, UK) with a software-controlled dynamometer. The optimized FU-CBD-G formulation was placed in a jar having a dimension of 40 mm height, and 55mm diameter. Whereas, the sample was filled to a height of 30 mm. Testing sample was kept flat to nullify the possibility of air bubble entrapment and early triggering of the test. FU-CBD-G was compressed at 1mm/s of compression rate for twice till 40% of the original height of gel by Compression platen. Data acquired by Texture profile analysis over the following conditions data acquisition rate, pre-test speed, test speed, post-test speed, trigger force, target mode distance, trigger type, and time-lapse between first and second compression was 200 points per second, 1.0 mm/s, 1.5 mm/s, 1.5 mm/s, 5 g, 10 mm, Auto and 5s respectively. Resultant force-time plots were obtained by analysis from which several mechanical properties such as adhesiveness, consistency, the force of adhesion, and hardness/firmness were inferred [42].

12. In- vitro drug release and Ex-vivo drug permeation studies

The In-vitro drug release and Ex-Vivo drug permeation studies were performed to evaluate and compare the permeation profile from 5-FU gel (conventional gel) with prepared FU-

CBD-G. A dialysis bag having a molecular weight of 12000 Dalton was used in the case of In-vitro studies while in the case of Ex-vivo studies excised, shaved rat skin was used. In In-vitro studies, dialysis membrane while in case of Ex-vivo studies excised skin was staged between donor compartment and acceptor compartment of Franz diffusion cell with 0.785 cm^2 of exposed area. PBS (Phosphate buffer saline) of pH 7.4 and volume of 10 mL of was filled in the receptor compartment and same was maintained at 37 ± 0.5 °C with continuous stirring throughout the experiment. 1.0 g of FU-CBD-Gel and conventional gel of 5-FU and CBD were spread on the mounted membrane in an even manner. The samples were withdrawn at specific time intervals of 0, 0.5, 1, 2, 4, 6, and 8 h from each receptor compartment. 0.5 mL of sample was withdrawn from the acceptor compartment at each predetermined time point and instantly fresh media of equal volume was added to the acceptor compartment to assure sink condition. The concentration of 5-FU, and CBD permeated from donor compartment to acceptor compartment was analyzed and measured by spectrophotometer in triplicate at the wavelength of 267 nm and 220 nm for 5-FU and CBD respectively using UV spectrophotometer (UV-1601 Shimadzu UV-visible spectrophotometer) [35]. The Amount of drug released from gel was calculated by equation 6 and the flux was calculated from linear portion of the slope of the cumulative amount of drug permeated versus time plot [5].

$$\text{Amount of drug Permeated} = \frac{\text{Conc.(µg/mL)x dilution factorX Vol.of release meium (ml)}}{\text{Permeation area(cm2)}} \text{..Equation 6}$$

13. Dermatokinetic study

The amount of drug deposition in different layers of the skin was analyzed by **a** dermatokinetic study. Excised and shaved skin samples were stuffed between donor and receptor compartments of the Franz diffusion cells. FU-CBD-G and conventional gel of 5-FU and CBD were spread in an even manner on the mounted membrane and each group consists of seven Franz diffusion cells. At each predetermined time interval of 0, 0.5, 1, 2, 4, 6, and 8 h mounted skin from a Franz diffusion cell was removed. Then, washing of obtained skin with normal saline was done to remove the formulation above the skin and then dipped in pre-heated water at 60˚C for 2-3 minutes to ease the separation of skin layers. Then, the Epidermis and dermis layer of skin were split up using forceps. Obtained layers were finely chop up into small pieces and to extract the drug from minced layers were then macerated in 5 mL of methanol for 24 hours. After maceration, samples were centrifugated at 5000 RPM at temperature of 4˚C for 10 minutes. then, methanol was collected from the supernatant and drug content from the collected supernatant was quantified using the prepared HPLC method.

All measurements were performed in triplicate. The concentration of 5-FU and CBD per cm square versus time was plotted for each formulation. Then Dermatokinetic parameters including $C_{skin\ max}$, $T_{skin\ max}$, and $AUC_{0\text{-}8\ h}$, of each formulation were calculated using PK solver software [49].

14. Statistics analysis

GraphPad prism software (version 8.0), San Diego, CA, USA was employed to perform statistical analysis. To check statistical significance of reported data Tukey-Multiple comparison was used with values of $P \leq 0.05$ which indicates that data is statistically significant along with one-way-analysis of variance (ANOVA).

15. Formulation development

Multiple emulsification method was employed for the preparation of FU-CBD-NLCs. The lipidic mixture was initially developed by adding 1% CBD in a melted 2% binary mixture consisting Gelucire 53/13 and coconut oil in ratio 6:4. Then, Aqueous phase was prepared by adding 1% of Smix. The Smix comprises of Tween 80 and Transcutol P mixed in ratio of 2:1. Primarily, 1% of 5-FU was added in 100µL of aqueous phase. Drug added aqueous phase was then added to the lipidic phase dropwise with continuous stirring keeping the temperature at 70°C. Next, the lipidic mixture was added to the aqueous phase under constant stirring at 800 rpm to obtain the NLCs, which is then stirred for next 30 minutes to stabilize the developed FU-CBD NLCs.

15.1 Characterization of developed formulation

15.1.1 Mean Particle size, zeta potential, and morphological examination

The size, PDI and surface charge of FU-CBD NLCs was analysed by using the Zetasizer (Malvern nano ZS, Inc. UK). Adequate amount of sample was diluted using Milli-Q water, filled in a cuvette and analysed in triplicate [39], [40]. The surface morphology of the FU-CBD NLCs was examined by the scanning electron microscope (SEM). For this, the diluted samples were placed on copper sputter, coated with gold-palladium and analysed after placing in sample inlet [41]. Transmission Electron Microscopy was performed using diluted samples placed on copper grid and analysing at high resolution at a scale of 200nm in a Transmission Electron Microscope. Captured images were investigated using Olympus Soft Imaging Viewer [42].

15.2 Entrapment Efficiency

The percentage entrapment efficiency (%EE) of 5-FU and CBD was determined by the previous established method [19] using equation 1. The developed FU-CBD-NLC was added into the aqueous phase and subjected to centrifugation for 20 minutes at 14000 RPM. The supernatant was then collected and the amount of free drug was determined at 260 nm and 220 nm for 5-FU and CBD, respectively. All the experiments were performed in triplicate for precise readings [7], [43].

$$(\%EE)\ \text{Percent Entrapment efficiency} = \frac{\text{Initial Drug (mg)} - \text{Free Drug(mg)}}{\text{Initial Drug (mg)}} \text{x } 100 \ldots \text{Equation 1}$$

Where, 'Initial drug' is the amount of drug used to prepare FU-CBD-NLCs and 'Free drug' is amount of drug present in supernatant layer

15.3 Preparation of FU-CBD NLCs gel

To prepare NLC gel, Carbopol 934 (1%) was added to water under continuous stirring overnight at 1200 RPM using a magnetic stirrer (Remi Motors Ltd., India). The base of Carbopol 934 was then neutralized using triethanolamine (0.05% w/w) for developing gel. The developed FU-CBD-NLC was then added to the gel under vigorous stirring. 0.01% benzalkonium chloride was finally added as preservative in the preparation [63,64].

16. Evaluation of FU-CBD NLCs Gel

The developed preparation was subjected to evaluation based on physical properties, homogeneity and pH. Then the properties such as extrudability, Spreadability and texture was determined.

16.1 Physical properties, homogeneity and pH

Consistency or any separation along with homogeneity was examined visually. The pH of the gel was determined by the pH meter (Microprocessor pH system, India). All experiments were performed in triplicate at 25 ± 1ºC. [25]–[27].

16.2 Extrudability and Spreadability

Extrudability and Spreadability of a gel are important properties. To evaluate the extrudability, the gel was filled in a collapsible tube. Pressure was applied on the tube 10 seconds so that to obtain a ribbon of 0.5cm. The extrudability of the gel was calculated using equation 2.

$$E = W/A \ldots \text{Equation 2}$$

Where, E, A, and W stand for extrudability, Area and applied weight to extrude gel from tube respectively.

The Spreadability was determined by the drag and slip properties of the gel. The gel was firstly poured on the lower slide, upon which the upper slide was placed, such that the slide

would have a balanced hook attached on top. The time taken by the upper slide to shift its position from its place when a known weight was added to the hook was recorded to determine the spredability using the equation 3 [25].

$$S = \frac{m \times L}{t}$$ ……. ……. Equation 3

Where S, L, t, and m represent Spreadability (g/sec.), fixed distance, time (s), and weight, respectively.

17. Depth permeation study by confocal laser scanning microscopy

The permeation and deposition of the drug are crucial parameters for better therapeutic dermal drug delivery[46][47][48]. To optimize permeation of prepared NLCs formulation and their deposition efficiency was validated using confocal laser scanning microscopy (Zeiss, Heidelberg, Germany). Simple gel and Rhodamine loaded NLCs gel were prepared by optimized formula. Briefly, rhodamine b was added instead of the drug in the formulation and carrier efficacy was observed. Rat skin was shaved and mounted between Franz diffusion cell and 1 g of rhodamine loaded NLCs gel and Control gel. Then, the prepared gels were spread on the mounted membrane in an even manner. The skin was removed after 8 hours and cleaned with PBS having pH 7.4 for removal of excess and remained formulation gel over the skin. Then, cleared skin was preserved in formaldehyde solution until processing. Obtained samples were sliced and fixed over glass slides. The prepared slides were then observed using confocal laser scanning microscope [49], [50].

18. Skin irritation studies

A skin irritation test was performed to determine any irritation caused by the prepared FU-CBD-NLC gel. As temperature rise is one of the major parameters to validate irritation [51], [52]. Conventional 5-FU gel was compared with the prepared FU-CBD-NLCs loaded Gel. Rats weighing 140-160 g were chosen for the skin irritation test. According to the guidelines the polypropylene cage was used for caging of animals issued by CPCEA and kept in standard laboratory. Animals were divided in two groups and each containing 3 rats. Group I was marked as control and conventional gel was applied for analysis, while group II was marked as treatment group and FU-CBD-NLC gel was applied for irritation test. One-gram respective gel was applied over a shaved area of 1 cm^2 on dorsal skin of the rat. The temperature of applied site of conventional gel and NLC gel was measured at predetermined points (5 min, 0.5, 1, 2, 4, 8,12 hours) of the skin by infrared camera FLIR i3, FLIR Systems, Inc. USA.

19. Skin Retention analysis by Gamma Scintigraphy

19.1 Radiolabeling of FU-CBD with ^{99m}Tc

Radiolabelling of 5-FU-CBD was accomplished by ^{99m} Technetium pertechnetate (^{99m}Tc) with the help of tin salt (stannous chloride) as a reducing agent. Briefly, 50 µL of stannous chloride solution of concentration 2mg/mL was added to the FU-CBD-NLCs suspension and after incubation of 10 minutes, 20 µCi of ^{99m} Technetium pertechnetate was followed by 30 minutes of incubation. Then, the percent of radiolabelled FU-CBD-NLCs was calculated by using the equation 1 [16], [53], [54].

$$\text{Radiolabeling efficiency} = \frac{\text{Counts on bottom X100}}{\text{Counts on top+ bottom}} \quad \text{.....Equation 1}$$

19.2 Optimization of radiolabeling efficacy

Optimization of Radiolabeling efficacy was performed to optimize the best quantity of additives to be used for conducting scintigraphy studies and to minimize the chances of failure of the experiment. The radiolabeling of FU-CBD NLCs was optimized by Design Expert Software (Stat-Ease Inc. Minneapolis) by employing the central composite rotatable design. Firstly, stannous Chloride (mg/mL), and incubation time (hr) were selected as independent variables with a range of 1-4 mg/mL and 0 – 3 hours respectively for optimization. Percent radiolabeling efficacy with maximum constraint was selected as dependent variables for optimization studies.

19.3 Gamma scintigraphy investigation

The skin retention behavior of radiolabeled FU-NLC was investigated in Healthy albino Wistar rats by the gamma scintigraphy method. Briefly, Radiolabeled NLCs were incorporated into the gel base and 1 g of prepared radiolabeled gel base was applied to the area of 1X1 cm of the dorsal region of previously shaved rats. The behavior, permeation, and retention of FU-CBD-G as a hot-spot point [55], [56].

20. HET-CAM irritation test.

The irritation potential of substances was determined by HET-CAM test commonly known as hen's egg-chorioallantoic membrane test [57]. Thus, to evaluate and compare the irritational effect of 5-FU solution with FU-CBD-NLCs HET-CAM test was performed. Briefly, fertilized Chicken eggs were purchased from a local poultry farm. The obtained eggs were subjected to incubation at 37.5 ± 5 °C with 50 ± 5 % RH throughout the study. On the ninth day, a small pore was drilled and a window was sliced on the outer shell of the incubated eggs. Six eggs were divided into two groups and group I was exposed to an incremental dose of conventional formulation till 4X of the therapeutic dose while the second group was exposed to an incremental dose (till 4X of prepared dose) of FU-CBD-NLCs. After each

incremental dose of conventional-dose and FU-CBD-NLCs vascular factors such as hyperemia and small areas of hemorrhage in developed veins in eggs were observed [57]–[61].

21. In-Ovo Tumor grafting and treatment

To determine the comparative efficacy of formulation in-Ovo experiment was conducted. In-Ovo tumor was grafted with slight modification as prescribed by Achkar et al. and Liedtke et al. Fertilized Chicken eggs were incubated at 37.5 ± 5 °C with 50 ± 5 % RH throughout the study. On the ninth day, a small pore was drilled and a window was sliced on the outer shell of the incubated eggs. The A431 cell line was well cultivated in DMEM medium with additionally supplemented with the help of 10% Fetal bovine serum and penicillin/streptomycin solution of one percent strength. Then, grown cells were detached using trypsinization, followed by washing with DMEM media and suspended in DMEM media without PBS to get cell suspension. 50 μL of cell suspension consisting of 2.0 x 105 cells of A431 cells was inoculated. All the inoculated eggs were randomly divided into four groups that is I, II, III, and IV which were control, positive control, conventional formulation, and FU-CBD-NLCs treatment (consists 0.5% 5-FU and 4.5% CBD) groups respectively. Dosing was done on days 11,13,15 and 17. On day 18 tumor sample was collected, washed with PBS, and preserved in a formaldehyde solution. Obtained tumors were washed, weighed, and processed for slide preparation for histological analysis [62], [63].

22. Procurement of animals and grouping

All animal experiments were performed by following to European Community guidelines for experimentation and use on animals. The experiments on Albino wistar rats weighing 100-150g were approved by the animal ethics committee from the Institutional Animal Ethics Committee (IAEC, registration number 173/Go/Re/S/2000/CPCSEA) of Jamia Hamdard, New Delhi, India bearing the protocol number 1738. Animal House Facility was used to obtain and house rats during study. The rats were given standard pellet diet with water and were kept in cages made up of polypropylene under maintained temperature and humidity of 24 ± 2°C, and 55 ± 5% respectively.

Albino wistar rats having average weight of 150g were selected for In-vivo studies. Rats were randomly divided into four groups i.e., GT-I, GT-II, GT-III, and GT-IV whereas each group consists of 9 rats. Group GT-I serves as normal control (rats were neither exposed to cancer inducing agents nor to formulation. Group-II serves as positive control where rats were only exposed to cancer inducing agents. Group-III serves as marketed gel treated it was exposed to

cancer inducing agents and then treated to the marketed formulation (1% FU gel), whereas Group-IV serves as treatment group which was treated formulation gel treated in this group rat were exposed to cancer inducing agents and then treated by FU-CBD-NLCs Gel.

22.1 Induction of tumor

Skin tumors were developed by reported method by Jyoti et. al 2015. Dorsal hair of rats was removed using surgical clipper and hair removal cream prior two days of initiation of experiment. On shaved skin 100µL DMBA (1µg /1µL acetone) was applied topically. After 14 days, tumor initiation was further promoted by croton oil seed applied topically thrice a week for next 14 weeks [64]. All rats were routinely observed for the appearance of skin tumor or skin papilloma and only tumor with a diameter greater than 2 mm, was taken into consideration for the evaluation.

22.2 Treatment pattern and analysis

When there is stable tumor appearance in the rats, the rats were divided as per plan and rats were treated as per treatment paradigm for 24 days. During the 24 days treatment regime tumor number, tumor volume, and tumor area, was recorded on day 3,6,9,12,15,18,21 and 24. Additionally, the systemic toxicity was investigated and discussed based on survival rate of the rats.

The tumor area and volume were calculated using equation 2 and 3 respectively. On 24th day of treatment the rats were humanely sacrificed. Treated area of the skin was removed which was used for histopathological evaluation and biochemical parameters estimation.

$$\text{Tumor Area} = \pi/4(\text{lenth X width}) \quad \text{..equation 2}$$

$$\text{Tumor Volume} = \pi/6(\text{lenth X width X height}) \quad \text{..equation 3}$$

22.3 Histopathology of skin

Skin tissues of sacrificed rats were obtained and processed for histopathological analysis to identify and compare histopathological changes of each group. Briefly, Skin samples were sliced into sections. Further, sliced sections were embedded in paraffin followed by hematoxylin and eosin dye staining. Later, the prepared stained sectioned slides were observed with the help of inverted microscope (Olympus, Japan) for analysis of histopathological changes in the samples [18].

22.4 Biochemical assay

Biochemical estimation such as catalase (CAT), Malondialdehyde (MDA), Superoxide dismutase and glutathione (GSH) were estimated from skin tissue homogenate from each group mentioned in in-vivo antioxidant study. Catalase and GSH are the enzymes which facilitate quenching of free radical, superoxide and peroxide radicals thus higher-level offer

defense against oxidative stress while reduced level of MDA indicates reduced lipid peroxidation. Briefly, excised skin was washed with ice cold phosphate buffer. Then the obtained washed tissues were finely chopped and then homogenized by with the help of Polytron Homogenizer (Kinematica Polytron, Luzem, Switzerland). Then, prepared centrifuged for a time period of 5 minutes at 3000 rpm resulting in separation of tissues. Then, supernatant was collected from the samples and used for biological estimation[65].

22.4.1. catalase (CAT)

Skin homogenate (0.2 mL) and 2mL of phosphate buffer having pH 7.4 was mixed together followed by the addition of hydrogen peroxide (0.95 mL). The obtained mixture was analyzed by using UV spectrophotometer at 240 nm wavelength[66]. CAT was calculated using equation 4.

$$\mu\text{moles of H202 decomposed/min/mg protin} = \frac{(\_A/\ \text{min})\ 1000x3}{\in \text{x mg protein}} \ldots\ldots\ldots\ldots\ldots \text{equation 4.}$$

22.4.2. Glutathione (GSH)

Skin homogenate (0.2 mL), 0.02 M EDTA (2 mL) and cold distilled water (1.6 mL). After mixing, 50% trichloroacetic acid (0.4 ml) was added. Then prepared solution was vigorously shaken using a vortex mixer for 10 minutes. Further, the obtained mixture was then centrifuged for 15 minutes at 3500rpm. Supernatant (2 ml) was collected and mixed with 4mL of Tris buffer of strength 0.4 M and having pH 8.9. Then, 0.1 mL of 5,5′-dithiobis- (2-nitrobenzoic acid) (DTNB) solution having strength 0.1 M was mixed with prepared solution. The resultant mixture was then analyzed by UV spectrophotometer at an absorbance of 412 nm. GSH content was calculated in terms of nanomoles of GSH per milligram of the protein [67]–[69]

224.3. Malondialdehyde (MDA)

Skin homogenate 0.2 mL was mixed with 0.2mL of 8.1% sodium dodecyl sulfate and followed by addition of 20% acetic acid (1.5 mL). then by using NaOH pH was adjusted to 3.5. after adjusting pH 0.8 percent thiobarbituric acid (1.5 mL) to form reaction mixture. Then, volume of the mixture was adjusted to 4mLby using distilled water. Then prepared were mixed properly and were kept in shaking water bath for a period of 60 minutes at maintained temperature 80°C. Tubes were carefully removed and kept in ice cold water for 10 minutes. Further, Butanol and pyridine mixture in composition of 30:2 ratio was prepared and 5 mL of it was added to obtained mixture followed by 1mL distilled water. Further, at 3000 rpm mixture was centrifuged for 15 minutes and organic phase as supernatant was collected.

Later, obtained supernatant was analyzed at an absorbance of 532 nm by UV spectrophotometer[65]. MDA was calculated by using equation 5.

$$\text{MDA content} = \frac{A}{\varepsilon l} DF \quad \text{.....equation 5.}$$

Where A, ε, l and DF stands for absorbance, extinction coefficient, light path, and dilution factor respectively.

22.4.4. Superoxide dismutase

Excised skin (200mg) was well homogenized in potassium phosphate buffer 2 ml of potassium phosphate of pH 6.8. Then, obtained homogenates were centrifuged at 1500 rpm for 10 min and obtained supernatant was collected. Then, supernatant was further assayed for SOD activity. Briefly, 100 µl of obtained supernatant was mixed with 25 µl of pyrogallol and volume was adjusted to 3mL Tris buffer having pH 8.5. Then, prepared solution was analyzed at 420 and effect of conventional gel with prepared FU-CBD-NLCs gel with control group was compared. The SOD value was denoted as U.mg-1 of protein [70][71].

23. RESULTS AND DISCUSSION

23.1. Initial Risk Assessment

A holistic method development practice was adopted for a systematic understanding of the method parameters influencing the method performance indicators. In this regard, the risk assessment study was performed for identifying the method parameters, where the method variables were assessed for their likely impact by assigning risk scores. Table **2** provides a list of method variables with their likelihood of impact on the method performance indicators, which indicates a high risk associated with mobile phase ratio and flow rate on peak area and peak tailing of the analytes

.

Table: 2 Risk estimation matrix (REM)

Method Performance Indicators	Risk Estimation Matrix (REM)					
	Mobile Phase Ratio	Mobile Phase pH	Sonication Time	Flow Rate	Oven Temp.	Injection Volume
Peak area	High	Low	Low	Mod	Low	Low
Peak tailing	High	Low	Low	Mod	Med	Med

High risk parameter Medium risk parameter Low risk parameter

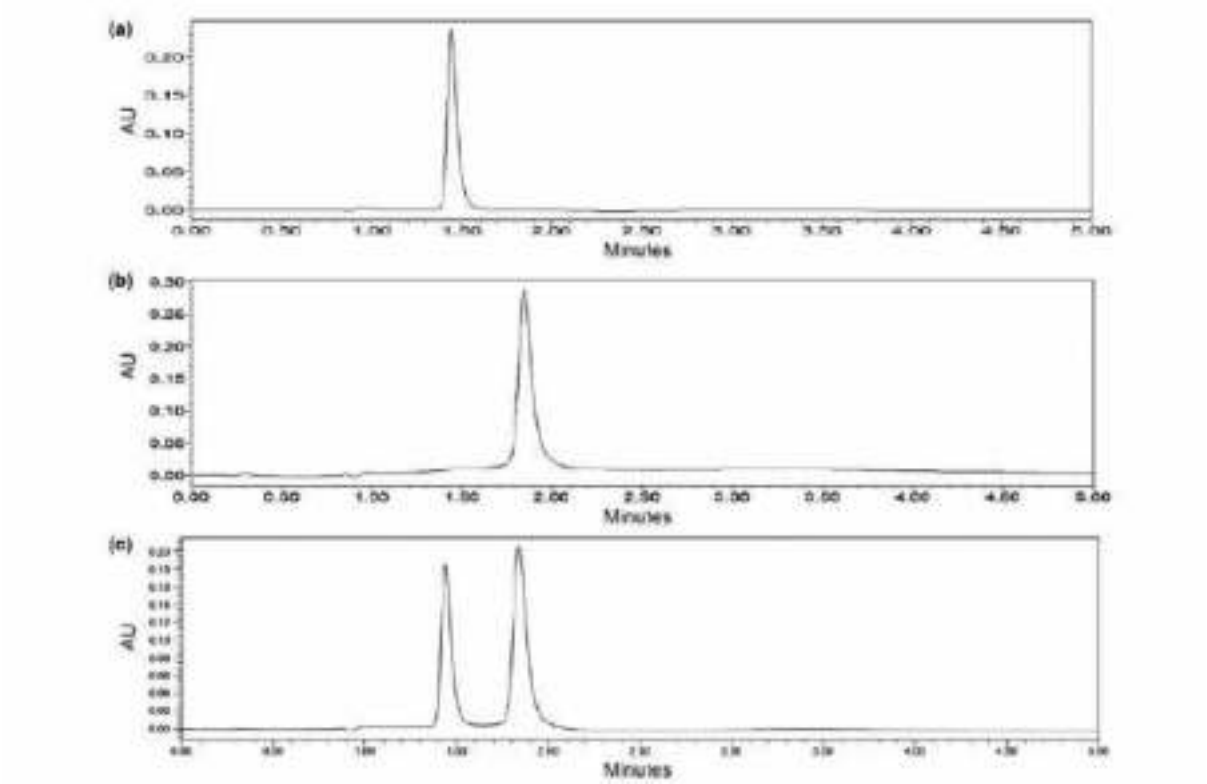

Fig. (1). Representative chromatogram of a) 5-Fluorouracil at λmax of 267nm, and b) Cannabidiol at λmax of 220 nm; c) Simultaneous determination of cannabidiol and 5-Fluorouracil at single wavelength, i.e., 237 nm, using optimized HPLC method).

23.2. Development and Optimization of the Method

Single wavelength was selected for analysis to make the prepared method more economical and realistic, which is based on the maximum absorbance of 5-FU and CBD at a single wavelength. UV spectra of methanolic solution of 5-FU as well as CBD, each having a concentration of 10 µg/ml, were obtained in the range of 400-200 nm. 5-FU exhibits maximum absorbance at 267 nm, while CBD shows maximum absorbance at 220 nm. Based on UV spectra, 237 nm was selected as a single wavelength which was further verified by PDA detector.

Mobile phases containing methanol or ACN and water in isocratic and gradient flow were tried for method development. The simultaneous detection of 5-FU and CBD was observed best in water: methanol gradient solution at a flow rate of 85% to 100% of methanol over 2.5 minutes, which then held at 100% methanol for 2 minutes at a flow rate of 0.75 ml/min as it produces high-resolution, sharp peaks with better separation of 5-FU and CBD. The retention time (RT) of 1.4 and 1.84 minutes was obtained for 5-FU and CBD, respectively. For comparison, both analytes (5-FU and CBD) were analyzed at their respective λmax, that is

267 and 220 nm, respectively (Figs. **1a** and **b**). 5-FU and CBD when analyzed simultaneously got separated at retention times of 1.4 and 1.84 minutes, respectively, which suggests that the retention time does not change of both drugs even in combination (Fig. **1c**). Overlay chromatograms of 5-FU and CBD were analyzed separately and simultaneously; the peaks of individual drugs got superimposed with the ones in combination. This indicates that there is no interaction of peaks of both analytes and it does not change their respective positions on simultaneous estimation (Fig. **2**). The prepared method for the analysis of 5-FU, CBD and their simultaneous determination suggests superiority over other methods as it is rapid, efficient and detects both analytes in just 4 minutes of run time. Similar elution time of 5-Fu was reported by Ahmad et al. [33].

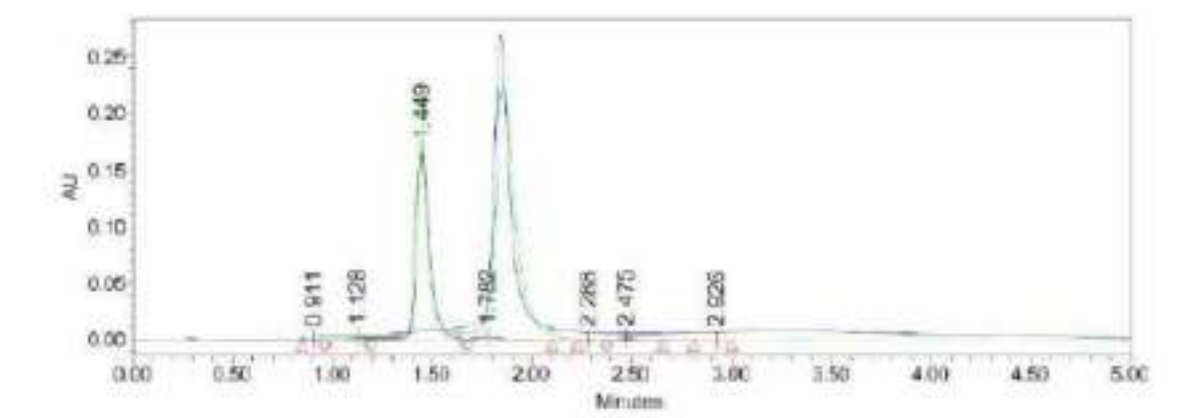

Fig. (2). Overlay chromatogram of **a**) 5-Fluorouracil at λmax of 267nm, and **b**) Cannabidiol at λmax of 220 nm; **c**) Simultaneous determination of cannabidiol and 5-Fluorouracil at single wavelength, i.e., 237nm, using optimized HPLC method.

23.3. Validation of Method in Plasma

Simultaneous detection of 5-FU and CBD in plasma was performed in water: methanol gradient solution with a flow rate of 85% to 100% of methanol over 2.5 minutes, which then held at 100% methanol for 2 minutes at a flow rate of 0.75 ml/min as it produces high-resolution, sharp peaks with better separation of 5-FU and CBD. 5-FU and CBD were found to be well separated with sharp peaks at retention times of 1.4 and 1.86 minutes, respectively. For comparison, both analytes (5-FU and CBD) were analyzed at their respective λmax of 267 nm and 220 nm, respectively, while simultaneous determination was performed at a single wavelength of 237 nm (Fig. **3**). Overlay chromatograms of 5-FU and CBD when analyzed separately and simultaneously were superimpoded, which suggests that there is no interaction of peaks of both the analytes and it does not change their respective positions on simultaneous estimation in plasma spiked samples (Fig. **4**). Obtained result shows linearity in

a concentration range of 10 to 100 µg/ml. The developed method can detect 5-FU and CBD separately, and when analyzed at a single wavelength, it can simultaneously detect 5-FU and CBD in plasma.

23.4. Method Validation

23.4.1. System Suitability Test

Relative standard deviation (RSD) of retention time and peak area for 5-FU and CBD was calculated after six successful runs; average retention time was found to be 1.40 ± 0.02 min and 1.83 ± 0.019 min with %RSD as 1.83% and 1.06% for 5-FU and CBD, respectively. The mean peak area of 5-FU and CBD was found to be 1159725.833 ± 16592 and 1881558.5 ± 26753 with %RSD values of 1.43% and 1.42%, respectively (Table 2). Obtained %RSD was less than 2% for retention time and peak area, which indicates suitability and reproducibility of prepared HPLC analytical method.

23.4.2. Specificity

By comparing chromatograms of a standard solution of 5-FU, CBD and FU-CBD with blank solution, the specificity of the prepared analytical method was determined. An injection volume of 10 µl of each standard sample was separately injected and analyzed. Retention times of 5-FU and CBD, when analyzed separately, were found to be 1.4 and 1.84 minutes, respectively. While in the FU-CBD mixture, retention times of 1.4 and 1.84 min were observed for 5-FU and CBD, respectively. Results revealed that the retention time of 5-FU and CBD did not change when analyzed separately and in combination, which suggests the specificity of the developed HPLC analytical method.

23.4.3. Linearity

Concentrations of 10, 20, 40, 80 and 100 µg/ml of 5-FU, CBD and FU-CBD were analyzed separately. 5-FU was analysed at 267 nm and CBD at 220 nm, while FU-CBD was analyzed at a single wavelength of 237 nm to evaluate linearity of prepared analytical HPLC method. Linear curve was obtained for 5-FU, CBD and FU-CBD when graph was plotted between concentration and peak area with correlation coefficient R2 value of 0.9852 for 5-FU, 0.9848 for CBD, while R2 values of 5-FU and CBD in FU-CBD analyzed at λmax of 237 nm were found to be 0.9823 and 0.9822, respectively (Fig. 5). Obtained result suggests that the prepared method showed linearity over the measured concentration range.

23.4.4. Sensitivity

To evaluate the sensitivity of prepared HPLC method, calibration curves were further used to analyze lowest amount of drugs that can be detected and quantified by HPLC (LOD and

LOQ). LOD was found to be 15.9 ng/ml and 13.24 ng/ml for 5-FU and CBD, respectively, at their respective λmax (267 nm for 5-FU and 220 nm for CBD) when detected separately. At common wavelength of 237 nm, LOD obtained was 16.91 ng/ml and 12.31 ng/ml for 5- FU and CBD, respectively (Table 4A). The lowest amount of drug that could be quantified (LOQ) was found to be 48.40 ng/ml and 40.13 ng/ml for 5-FU and CBD at their respective λmax of 267 nm and 220 nm, respectively. At 237 nm, 51.25ng/ml and 37.32 ng/ml of 5-FU and CBD, respectively, could be quantified by the developed HPLC method (Table 4B). The obtained result suggests the method to be highly sensitive and that it can quantify small amounts of drug which would be useful in various studies, such as calculation of entrapment efficiency, in-vitro release, ex-vivo release, in-vivo drug biodistribution and pharmacokinetic studies.

Table.3. Sensitivity study

Analyte	Slope	Standard Deviation	LOD	LOQ
At Individual λmax (267 nm for 5-FU and 220nm for CBD)				
5-FU	46836	226711.3	15.9731691	48.40853089
CBD	50857	204126.7	13.2453971	40.13738522
At Single Wavelength (257 nm)				
5-FU	40142	205763.8	16.9154636	51.2589862
CBD	53945	201330.8	12.3160951	37.32149411

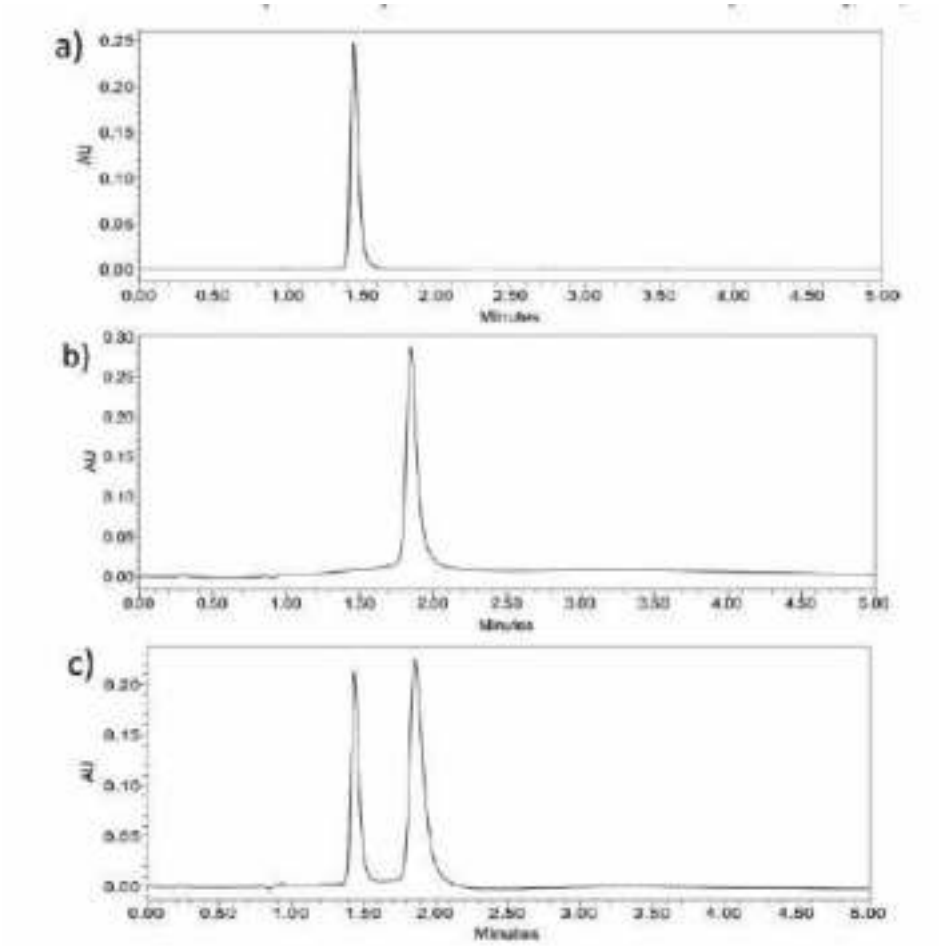

Fig. (3). Representative chromatogram of detection in plasma of **a**) 5-Fluorouracil at λmax of 267nm, and **b**) Cannabidiol at λmax of 220 nm; **c**) Simultaneous determination of cannabidiol and 5-Fluorouracil at single wavelength, i.e., 237nm, using optimized HPLC method.

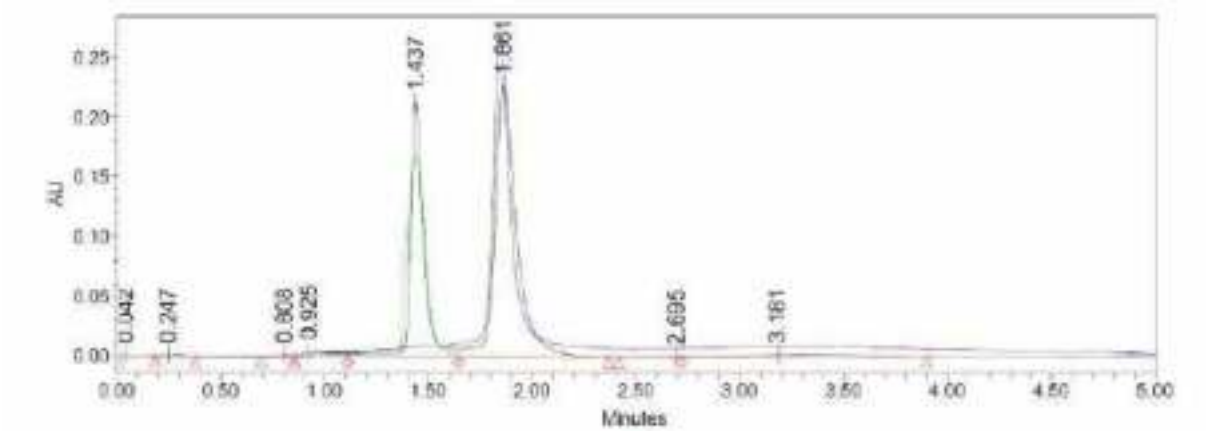

Fig. (4). Overlay chromatogram of plasma spiked samples of **a**) 5-Fluorouracil at λmax of 267nm, and **b**) Cannabidiol at λmax of 220 nm; **c**) Simultaneous determination of cannabidiol and 5-Fluorouracil at single wavelength, i.e., 237nm, using optimized HPLC method.

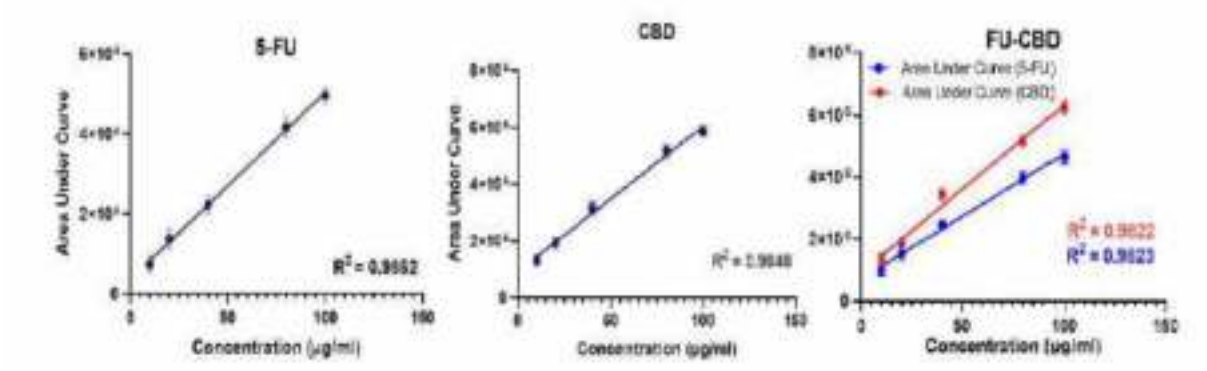

Fig. (5). Area under the curve at different concentrations of a) Cannabidiol at λmax of 220nm, and b) 5-Fluorouracil at λmax of 267nm; c) Simultaneous determination of cannabidiol and 5-Fluorouracil at single wavelength, i.e., 237nm, using optimized HPLC method.

Table 4. (A) System suitability for 5-FU at single wavelength, i.e., 237 nm; (B) System suitability for CBD at single wavelength, i.e., 237 nm.

(A) System Suitability for 5-FU at 237 nm		
System Suitability Parameters	Retention Time	Peak Area
Run 1	1.43	1162575
Run 2	1.37	1157652
Run 3	1.39	1134854
Run 4	1.41	1185489
Run 5	1.43	1152548
Run 6	1.38	1165241
Mean	1.401666667	1159725.833
Standard deviation	0.025625508	16592.26472
Relative standard deviation (RSD)	1.828216989	1.430697174
(B) System Suitability for CBD at 237 nm		
System Suitability Parameters	Retention Time	Peak Area
Run 1	1.81	1900678
Run 2	1.84	1945182
Run 3	1.87	1899527
Run 4	1.84	1936826
Run 5	1.83	1882565
Run 6	1.84	1724573
Mean	1.838333333	1881558.5
Standard deviation	0.019407902	26753.46791
Relative standard deviation (RSD)	1.055733572	1.421878082

23.4.5. Ruggedness

Ruggedness test was performed to check the reproducibility of results on different HPLC with the same analyst and on the same HPLC with different analysts. The recovered concentration of 5-FU, when analyzed by HPLC-1 at 237 nm, was found to be 9.54 ± 0.08, 19.58 ± 0.27 and 29.77 ± 0.20 µg with percent recovery of 95.46, 97.90 and 99.26%, respectively, while concentration of 5-FU when analyzed by HPLC-2 by the same analyst at 237 nm was found to be 9.52 ± 0.10, 19.63 ± 0.13 and 29.71± 0.28 µg with percent recovery of 95.22, 98.17 and 99.06% at theoretical concentration of 10, 20, and 30 µg/ml, respectively. Recovered concentration of CBD when analyzed by same analyst on HPLC-1 at 237 nm was found to be 9.7 ± 0.3, 19.37 ± 0.64 and 29.29 ± 0.34 µg with percent recovery of 97.44, 96.86 and 97.63%, respectively, while same samples when analyzed by same analyst on HPLC-2 recovered concentration were calculated as 9.5± 0.2, 19.65 ± 0.31 and 29.36 ± 0.18 µg with percent recovery of 95.01, 98.28 and 97.88% at theoretical concentration of 10, 20, and 30 µg/ml, respectively, as illustrated in Table 5(A). Recovered concentration of 5-FU, when analyzed by HPLC-1 by analyst-1 at 237 nm, was found to be 9.7 ± 0.48, 19.77 ± 0.30 and 29.66 ± 0.46 µg with percent recovery of 97.42, 98.89 and 98.87%, respectively, while concentration of 5-FU when analyzed by analyst-2 on HPLC-1 at 237nm was found to be 9.6 ± 0.35, 19.81 ± 0.13 and 29.63 ± 0.22 µg with percent recovery of 96.08, 99.06 and 98.79% at theoretical concentration of 10, 20, and 30 µg/ml, respectively. Recovered concentration of CBD when analyzed by analyst-1 at HPLC-1 at single wavelength, i.e., 237 nm, was found to be 9.86 ± 0.30, 19.50 ± 0.09 and 29.40 ± 0.11 µg with percent recovery of 98.67, 97.15 and 98.00%, respectively, while same samples when analyzed by analyst- 2 on HPLC-1 recovered concentration were calculated as 9.57 ± 0.31, 19.67 ± 0.33 and 29.51 ± 0.53 µg with percent recovery of 95.75, 98.35 and 98.39% at theoretical concentration of 10, 20, and 30 µg/ml, respectively, as illustrated in Table 5(B). The obtained results show high degree of ruggedness and prepared HPLC method to be reproducible on different HPLC systems and by different analysts. Obtained validation results are in accordance with the literature [34-36].

Table 5. (A) Ruggedness data of 5-FU and CBD in different HPLC instruments with the same analyst analyzed at single wavelength, i.e., 237 nm; (B) Ruggedness data of 5-FU and CBD by different analysts in same HPLC instrument analyzed at single wavelength, i.e., 237 nm.

(A) Ruggedness Data of 5-FU and CBD in Different HPLC Instruments with the Same Analyst Analyzed at a Single Wavelength, i.e., 237 nm.					
Drug	Theoretical Concentration µg/ml	Recovered Concentration		% Recovery	
		HPLC-1	HPLC-2	HPLC-1	HPLC-2
5-FU	10	9.91 ± 0.08	9.52 ± 0.10	99.46	95.22
	20	19.58 ± 0.27	19.63 ± 0.13	97.90	98.17
	30	29.77 ± 0.29	29.71 ± 0.28	99.26	99.06
CBD	10	9.7 ± 0.3	9.5 ± 0.2	97.44	95.01
	20	19.37 ± 0.64	19.65 ± 0.31	96.86	98.24
	30	29.29 ± 0.54	29.36 ± 0.18	97.63	97.88
(B) Ruggedness Data of 5-FU and CBD by the Different Analysts in the Same HPLC Instrument Analyzed at a Single Wavelength, i.e., 237 nm.					
Drug	Theoretical Concentration µg/ml	Recovered Concentration		% Recovery	
		Analyst-1	Analyst -2	Analyst -1	Analyst -2
5-FU	10	9.7 ± 0.48	9.6 ± 0.35	97.42	96.08
	20	19.77 ± 0.20	19.81 ± 0.13	98.89	99.06
	30	29.66 ± 0.06	29.63 ± 0.22	98.87	98.79
CBD	10	9.86 ± 0.30	9.57 ± 0.31	98.67	95.75
	20	19.50 ± 0.09	19.67 ± 0.33	97.15	98.35
	30	29.40 ± 0.11	29.51 ± 0.53	98.00	98.39

24. Application of the Analytical Method for Pharmaceutical Nanoformulations

The percentage entrapment efficiency of 5-FU and CBD in prepared FU-CBD-L, FU-CBD SLN and FU-CBD NLC was analyzed by prepared analytical method at a wavelength of 237 nm. The percent entrapment efficiency of 5-FU and CBD was found to be 64.5% and 76.8% in FU-CBD-L, 73.4% and 81.2% in FU-CBD SLN, while 75.8% and 86.6% in FU-CBD NLC, respectively. Results revealed NLC to have maximum drug entrapment compared to liposome and SLN. This might be due to the presence of solid as well as liquid lipid, which enhances the solubility of the drug and the formation of the matrix system. The prepared method did not show any significant changes in drug peak, retention times, and no extra peak was observed, which assures selectivity and high specificity.

25.In-silico binding capacity analysis

The molecular docking study confirmed the selectivity and potency of Cannabidiol and 5-Fluorouracil when interacted with the active site of the target protein p38 MAP kinase (PDB ID: 2GTM). Both the compound Cannabidiol and 5- Fluorouracil showed excellent dock scores of -9.27 Kcal/mol and -7.54 Kcal/mol respectively. Both the compound has demonstrated strong interaction within the binding site of protein with hydrogen and hydrophobic bond interaction as shown in Figure 6a and b and Table-6. 5- Fluorouracil forms a strong hydrogen bond with Met109 and Gly110 amino acid residue with hydrogen bond lengths of 2.30 and 2.21Å respectively (Figure 6c), another compound Cannabidiol also forms a hydrogen bond with Hie107 amino acid residue with a bond length of 2.12 Å (Figure 6d). Orientation of both the compound was found little different, however interaction is very strong and both the compounds are tightly bounded to the active site of binding pocket (as shown in Figure 6e) demonstrating prominent inhibitory activity of lead compounds. The study confirms the selectivity and potency of 5-FU and CBD to interact with target protein p38 mitogen-activated protein kinase (MAPK). p38 MAPK pathway subsequently activates activator protein-1 (AP-1) which leads to activation of transcription factor and COX-2 expression. Furthermore, AP-1 and COX-2 are known to play functional roles in skin carcinogenesis. As p38 MAPK plays important role in cell apoptosis but it has been well known for multidrug resistance (MDR) in cancer cells [9]. It is already reported in the literature that long-term exposure to 5-FU in skin cancers leads to chemoresistance. Thus, to overcome the chemoresistance and achieve a better therapeutic effect combination of 5-FU and CBD could be a new horizon. Both compounds bind strongly with a hydrogen bond to p38 MAPK with a good docking score which indicates the combination of 5-FU and CBD in a single dose will not only eradicate the chemoresistance of 5-FU but also greatly enhance the in-vivo efficacy of 5-FU in combating skin cancer.

Table 6: Dock score and Interaction of Cannabidiol and 5 FU p38 MAP kinase (PDB ID: 2GTM)

			Interactions		
Drug	**Dock Score (kcal/mol)**	**H-bond Length (°A)**	**Hydroge n Bond**	**Hydrophobic**	**Other**
5-Flourouracil	-9.27	2.30 2.21	MET109 GLY110	VAL38, ALA40, VAL30, LEU113, ALA111, LEU108, ILE84, ALA51, LEU156, ALA157, VAL158, LEU167, LEU171	Polar: HIE107, THR106, SER154, ASN155, ASN115, HIS174
Cannabidiol	-7.54	2.12	HIE107	VAL30, ALA40, VAL38, LEU171, PHE169, LEU167, ILE84, LEU86, LEU104, LEU75, LEU108, MET109, ALA111, VAL158, ALA157	Polar: THR106, SER154

26. Compatibility Analysis

The FTIR spectra of 5-FU show characteristic peaks at 3120.66 cm^{-1}, and 3064.60 cm^{-1} were observed representing Imide stretching (-NH) i.e., Imide I and Imide III respectively. The peaks at 2921.66 cm^{-1} to 2993 cm^{-1} showed -CH stretching vibrations while -CH bending vibrations were observed at 1644.90 cm^{-1}. The sharp peak observed at 1720.12 cm^{-1} was observed representing the presence of the Carbonyl (-C=O) group. the alkyl halide group i.e., -CF group in the structure of 5-FU shows a peak at 1242.63 cm^{-1} to 1179.30 $cm^{-1,}$ and the disubstituted Aromatic ring is shown a characteristic peak at 747.02 cm^{-1} (Figure 6f).

The FTIR spectra of CBD are represented in Figure 6g. Spectra show the characteristic peak at 723.42 cm^{-1} showing the presence of a Disubstituted aromatic ring. The peaks at 2854.44 represent -CH stretching vibrations while, -CH bending vibrations were observed at 1456.66 cm^{-1} to 1720 cm^{-1}. The free -OH groups were observed at 2923.31 cm^{-1}.

All the peaks that were observed in individual spectra of 5-FU and CBD were also observed in the Spectra of the mixture indicating the compatibility of both the drugs shown in Figure 6h.

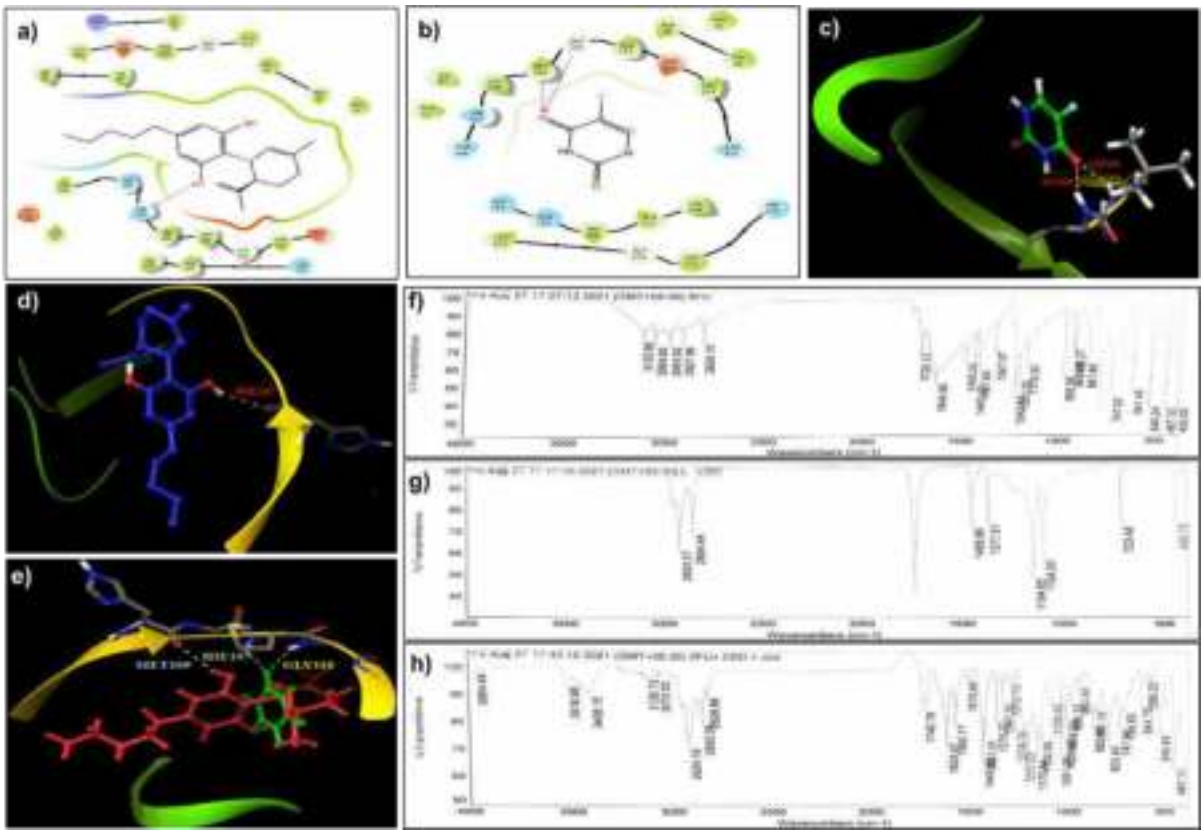

Figure 6: Representation of 2D dock poses, hydrogen and hydrophobic bond interaction of Cannabidiol and 5-Flourouracil with crystal structure of p38 MAP kinase (PDB ID: 2GTM) (a and b). Hydrogen bond interaction formed between Cannabidiol and 5-Flourouracil with co crystal is shown in pink solid line, hydrophobic and polar interactions are presented in green and blue colour respectively. The region in c and d shows 3D binding poses, hydrogen and hydrophobic bond interaction of 5-Flourouracil and Cannabidiol with crystal structure of p38 MAP kinase (PDB ID: 2GTM). The co-crystal is shown in grey and white stick model and the compounds (5-Flourouracil and Cannabidiol) is presented in green and blue ball and stick models; hydrogen bonding is shown in yellow dotted line. Superimposed structure of both the compounds, 5-FU is shown in green and Cannabidiol is presented in red ball stick model are represented as e. Representation of FT-IR spectra of 5-FU (f), CBD (g), and mixture of 5-FU and CBD (h).

27. Screening of Excipients

Optimizing of excipients plays a prime role in formulation development. Firstly, solid lipid was screened on basis of solubility of 5-FU in different solid lipids. The solubility of CBD was not considered for screening because it exhibits free solubility in lipids. The decreasing order of solubility of 5-FU was as follows Gelucire® 50/13 > Gelucire® 44/14 > precirol® ATO 5 > Geleol™ > compritol® 888 ATO shown in Figure 7a. After selection of solid lipid,

liquid lipids were screened and it was found that coconut oil exhibited maximum solubility of 7.9 ± 0.3 mg/mL followed by Labrasol®, Campul®, capryol® 90, Oleic Acid, Olive oil, and Castor oil respectively with the solubility of 7.3 ± 0.3, 5.8 ± 0.2, 5.8 ± 0.2, 2.1 ± 0.3, 0.8 ± 0.4, 0.6 ± 0.3 mg/mL respectively (summarized in Figure 7b). Thus, Gelucire® 50/13 and coconut oil were selected as solid-lipid and liquid-lipid respectively. After selection of solid-lipid and liquid-lipid, binary mixtures were prepared and any separation of in binary mixture was observed. No separation was observed in 1:0, 9:1, 8:2, 7:3, and 6:4, none of the binary mixtures imparts oil on filter paper except 5:5 thus, it was excluded from further analysis. Binary mixtures 9:1, 8:2, 7:3, and 6:4 was subjected to DSC analysis and the crystallinity index was calculated (illustrated in Figure 7d and 7e-i). It was found that as the ratio of liquid lipid in the binary mixture increases the enthalpy of the melting point decreases as compared to pure solid lipid. The binary mixture of ratio 9:1 shows a crystallinity index of 98% while there was a sharp reduction in crystallinity index in a binary mixture having ratio 8:2 and it gets reduces to 33% in binary mixture of ratio 6:4. Thus 6:4 was selected as a binary mixture for preparing FU-CBD-NLCs as it shows the least crystallinity index. Ali Sartaj et. Al reported similar parameters and results for the selection of binary mixtures [72]. As high amount of oil affects the rigidity of solid lipid matrix hence low melting point (Gibbs–Thomson effect) that may give supercooled nanoparticles. Gibbs–Thomson effect is more pronounced in nanosize system because of large ratio of specific area to volume [15]. Further, screening of surfactants and co-surfactants was carried out on basis of the emulsification capacity of each surfactant to emulsify the selected binary mixture. Higher the emulsification capacity of surfactant would lead to stable formulation development with a lesser amount of surfactant. The increasing order of emulsification potential of screened surfactant was Poloxamer 188 < Pluronic F127 < PEG 300 < PEG 400 < Tween 20 < Transcutol P < Tween 80 as shown in Figure 7c. The tween 80 shows maximum transmittance of 96% followed by Transcutol P (88%). Thus, Tween 80 and Transcutol P was selected as surfactant and co-surfactant respectively. After screening of surfactant and co-surfactant their optimum ratio to be used in the formulation was screened on basis of the emulsification potential of each Smix having concentrations of 1:1, 2:1, 3:1, 4:1, and 5 :1 of surfactant and co-surfactant respectively. The descending order for emulsification potential for screened Smix was 2:1 > 4:1 > 5:1 > 3:1 > 1:1. The Smix ratio 1:1, 2:1, 3:1, 4:1, and 5 :1 shows percentage transmittance of 85, 97,93,95,94 % respectively. Thus, Smix of ratio 2:1 was selected for formulation development as it shows maximum transmittance which will lead to the preparation of stabilized formulation.

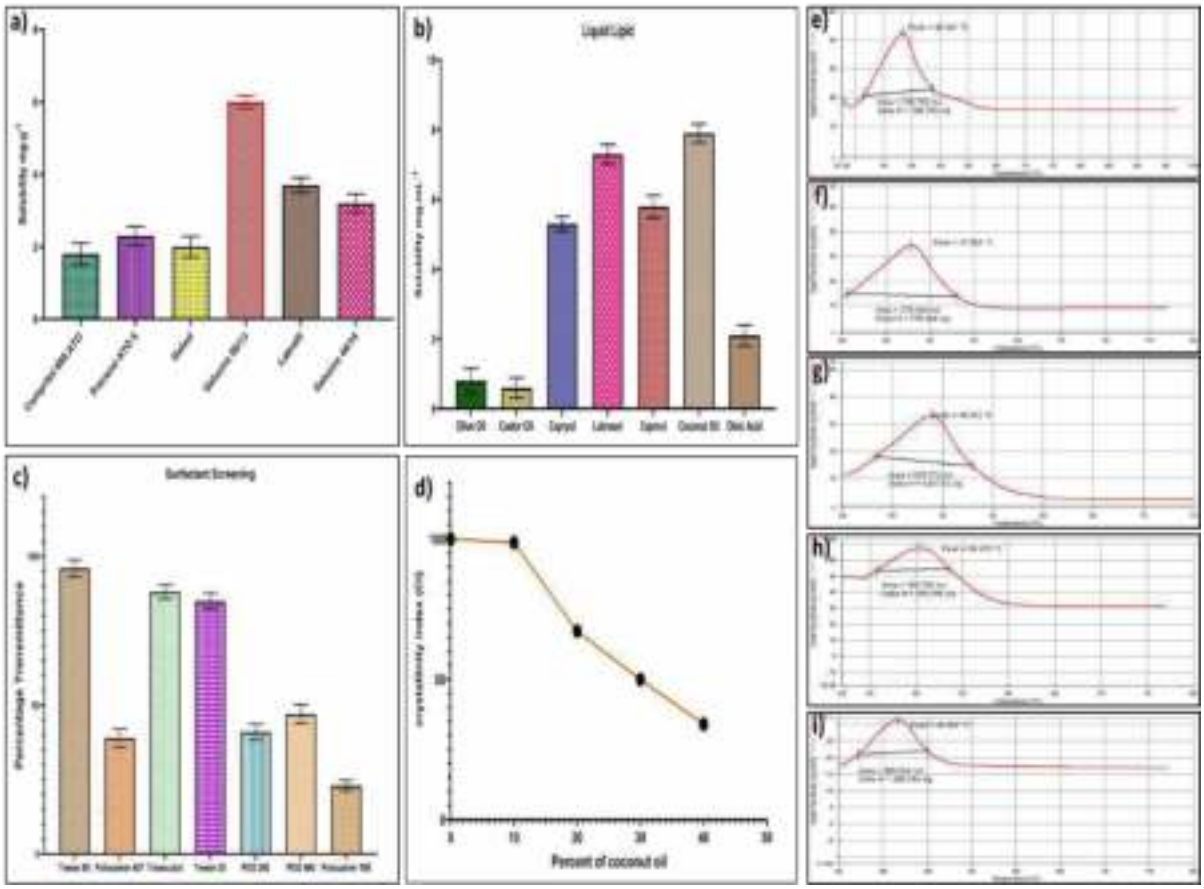

Figure 7: Representation of solubility of 5-FU in various solid lipids (a) and liquid lipids (b), screening of various surfactant to emulsify the selected binary mixture (c). Graphical representation of crystallinity index analysis at increasing concentration of liquid lipid to finalize binary mixture ratio. Representation of DSC Thermograms of Gelucire 100% w/w ©, BM with 10% w/w liquid lipid (f), BM with 20% w/w liquid lipid (g), BM with 30% w/w liquid lipid (h), and BM with 40% w/w liquid lipid (i).

28. Formulation optimization

It is essentially important to choose a suitable design for optimizing and characterizing a pharmaceutical preparation. The demonstration of variables frequently ends as a quadratic surface model. Therefore, for a kind of interpretation, the central composite design could be an excellent tool[73]. The effect of two independent variables (X1= Binary mixture and X2= Smix) was ascertained on dependent variables (Y1 = Particle Size (nm), Y2 = Polydispersity Index (PDI), Y3=%Entrapment efficiency of 5-FU, Y4 = %Entrapment efficiency of CBD) and the results were determined statistically using ANOVA. In correspondence with all four responses, the model is found to be fit to use for suggested models. The quadratic values (%CV, SD, and R^2) of the dependent variables are demonstrated in Table 7.

Table 7 Response analysis of dependent variables on different combination of independent variables and Summary of regression analysis for responses Y1, Y2 and Y3 against Independent variable X1 and X2 in Quality by design analysis

Runs	**Independent Variables**		**Dependent Variables**			
Formulations	X1: Binary Mixture	X2: Smix	Y1: Particle Size	Y2: PDI	Y3: % Entrapment efficiency of 5-FU	Y4: % Entrapment efficiency of CBD
F1	3	0.5	985	0.41	68.45	96.8
F2	2	1.25	202	0.13	84.12	98.2
F3	1	2	93	0.09	73	92.08
F4	3.41421	1.25	631	0.34	74.13	97.8
F5	1	0.5	368	0.27	75.9	89.25
F6	2	1.25	212	0.16	83.62	98.1
F7	0.585786	1.25	68	0.1	72.19	86.2
F8	3	2	297	0.26	82.01	98.8
F9	2	0.18934	896	0.33	73.34	94.5
F10	2	1.25	213	0.15	84.9	98.4
F11	2	1.25	206	0.13	83.56	98.7
F12	2	2.31066	208	0.18	80.45	98.7
F13	2	1.25	199	0.16	83.34	98.4
Quadratic model		**R^2**	**Adjusted R^2**	**Predicted R^2**	**% CV**	
Y1 Response		0.9993	0.9989	0.9961	2.82	
Y2 Response		0.9717	0.9516	0.8395	10.83	
Y3 Response		0.9952	0.9918	0.9884	0.6553	
Y4 Response		0.9954	0.9921	0.9731	0.3833	

28.1 Effect of the independent variable on the size of the particle

For efficient disposition of the drug in the skin and enhanced permeation, the size of the particle plays a crucial role. The size of particles thus should lie within the range of 100 to

200nm. The quadratic equation 12 was obtained which had variable attributes on the results. After employing the model, the following equation 12 engendered:

Particle size (Y1) = +206.40 + 202.15 A- 242.00B -103.25 AB + 67.80A^2 + 169.05 B^2……*Equation 12*

The predicted R^2 (0.9961) is found to be in reasonable agreement with the adjusted R^2 value which was 0.9989, suggesting a difference of less than 0.2. The results proposed a positive impact of binary mixture [Solid lipid: Liquid lipid (A)] on particle size. As the concentration of binary mixture increases, the size of the particle also elevated, while, in contrast to this, Smix (B) had a contrary effect. As the concentration of surfactant: co-surfactant increased, the particle size declined, this is due to the depletion in interfacial tension at the lipid to water interface (shown in Figure 8a and b).

28.2 Effect of the independent variable on the PDI

The design expert model suggested 17 runs in total which showed a PDI range between 0.09-0.41. The effect of binary mixture and Smix were used for investigating the quality attributes including PDI. For PDI, the quadratic equation 13 was attained that demonstrated the effect of terms:

PDI (Y2) = +0.1460 + 0.0812 A – 0.0678 B + 0.0075 AB + 0.0420 A^2 + 0.0595 B^2……. *Equation 13*

The software established the reasonable agreement between **Adjusted R^2 (**0.9516) and **Predicted R^2** (0.8395), for which the difference is again less than 0.2.

An increase in concentration of A and B there is increased the PDI, but as the concentration of Smix is increased there is prompt reduction in PDI was observed and shown in Figure 8c and d.

28.3 Effect of the independent variable on the entrapment efficiency of 5-FU and CBD

The clinical efficacy of a nano preparation could be delivered if the desired dose is achieved. The entrapment efficiency of all the prepared NLCs was investigated that found in the range of 68.45 to 84.9 % in the case of 5-FU whereas, for CBD, the entrapment efficiency ranges between 92.08- 98.8%. The predicted R^2 value was found to be in reasonable agreement with the adjusted R^2 and the difference was less than 0.2. The below-mentioned equation 14 and 15 was obtained that demonstrated the effect of terms on EE.

Y3 = +83.91 + 0.5379 A + 2.59 B + 4.12 AB – 5.42 A^2……. *Equation 14*

Y4 = +98.36 + 3.83 A +1.35 B – 0.2075 AB – 3.20 A^2 – 0.8969 B^2……. *Equation 15*

The lipid concentration had a favorable impact on entrapment efficiency while surfactant had a contrary effect. As the lipid concentration is increased, the solubility of the drug also

elevated which in turn increased the entrapment efficiency of the drug. However, an increase in surfactant concentration leads to a decline in the particle size providing more impact on the drug entrapment. The model was found to be highly significant as established by ANOVA statistical analysis (shown in Figure 8e-g).

29. Characterization

The optimized FU-CBD-NLCs (formulation F2 from table 7) were initially characterized by particle size analysis and it was found mean Hydrodynamic diameter of FU-CBD-NLCs was discovered to be 206.6 nm having a polydispersity index (PDI) of 0.164 (Figure 8i). The size of the particles indicates that it was suitable for transdermal drug delivery and the PDI value indicates that the prepared entire population of FU-CBD-NLCs nanodispersion was uniformly produced. The achieved nanonized particles with enhanced encapsulation of 5-FU and CBD within the lipidic core were anticipated to ease the transport of 5-FU and CBD in dermal and epidermal layers of skin. NLCs will provide a better accumulation of both drugs to the target site. Additionally, nanosized particles will be able to permeate through the cyst of skin cancer [74]. The zeta potential of FU-CBD-NLCs was found to be -34.5 mV (Figure 8j) which was attributed due to the presence of lipids, surfactants, and co-surfactant. The high value of zeta potential indicates FU-CBD-NLCs dispersion was stable and was less susceptible to form aggregates. The particle size results of FU-CBD-NLCs were further validated using Scanning electron microscopy (SEM) and transmission electron microscopy (TEM) analysis shown in Figure 8k and l, respectively. The analysis showed that prepared FU-CBD-NLCs were smooth and spherical in size and most of them were around 200 nm which was suitable for dermal drug delivery.

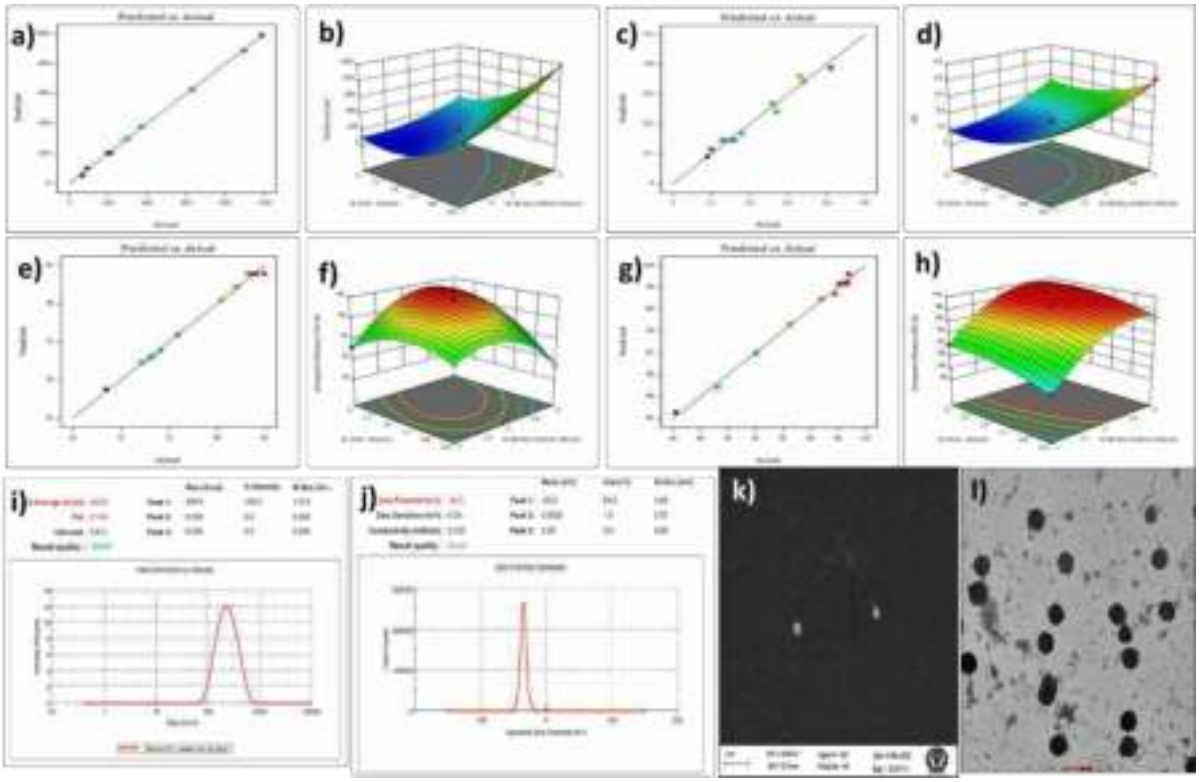

Figure 8: a-h represents optimization of prepared formulation. Whereas, a, c, e and g depict the relationship between the actual and predicted R-square values of independent factor after QbD analysis. b, d, f and h represents effect of independent variables (binary mixture and surfactant concentration) on dependent variables particle size, PDI, Entrapment efficiency of FU and entrapment efficiency of CBD respectively. i-l represents characterization of prepared FU-CBD-NLCs where zeta size and PDI analysis graph (i)zeta potential graph (j) and micrographs for morphological examination of FU-CBD-NLCs- SEM and TEM (k and l) are shown, respectively.

29.1 Differential Scanning Calorimetry analysis

The DSC investigation reveals that 5-FU and CBD exhibited a maximum peak at 286°C and 68°C respectively (shown in Figure 9a and b). It was observed that FU-CBD-NLCs, exhibit peaks at 50˚C, 67˚C, and 284˚C which are attributed to the binary mixture, CBD, and 5-FU respectively (Figure 9c). Result obtained in DSC analysis shows no interaction was there between both drugs and among the excipients. The formulation was stable and the presence of peak of CBD and 5-FU indicates both the drugs were well encapsulated in nano-particles.

29.2 X-ray diffraction studies

XRD spectra investigation was performed to confirm the structural conformation. 5-FU, CBD, and FU-CBD-NLCs. The 5-FU shows characteristic peaks between 10-40 of 2-theta. Specifically, the main peak of 28 of 2-Theta, while CBD shows a characteristic peak between 10-40 of 2-theta. Both CBD and 5-FU show a crystalline nature with sharp peaks which is attributed to the purity of the drug and their crystalline nature. The Binary mixture upon

analysis manifested its main peak of 3h between 5-35 of 2-Theta, specifically, the main peak for the binary mixture was found to be 19 and 23 of 2-theta as shown in Figure 9d-g. In XRD spectra of formulation, there was no characteristic peak of 5-FU and CBD instead it shows a similar peak of binary mixture which is attributed to the good encapsulation of the 5-FU and CBD between the structures of the crystal lattice of complexed lipid, thereby resulting in the modifications in the crystallinity of FU-CBD-NLCs from crystalline form to an amorphous form.

30. In-Vitro Cell line studies

30.1 Assessment of cytotoxicity of prepared formulation

Before proceeding to the in vivo anti-cancer study, it is highly essential to evaluate the cell cytotoxicity of different formulations at variable concentration levels. The human epidermoid carcinoma cell line (A431) was treated with 5-FU, CBD, FU-CBD, and FU-CBD-NLC that showed concentration-dependent cell cytotoxicity. The results exhibited IC_{50} at 91.48 µM, 75.22 µM, 59.73 µM, and 17.61 µM for CBD, FU-CBD, NLC-FU-CBD, and 5-FU, respectively (Figure 9h-k). As observed, the IC_{50} value of NLCs is, however, greater than 5-FU as it is a potent anti-cancer agent which hinders the thymidylate synthase activity promoting apoptosis of cells but is less than the non-NLC preparation. Placebo, on the other hand, showed 100% cell viability, which is consistent with the previously published results. As shown in the Figure 9h-k, after 48 hours, the viability of cancer cells decreased with an increase in concentration followed by a higher decline in the viability of cells treated with NLC-FU-CBD. Such a profound effect in comparison to 5-FU was due to the combination therapy of 5FU with CBD. The credit for effectiveness in therapy could also be attributed to the structure of NLC that escorted the lipid carrier into the cells via endocytosis releasing more amount of the drug in vitro. A study published in 2021 demonstrated the NLC hybrid of Docetaxel and Lidocaine gel increased the death of tumor cells [75].

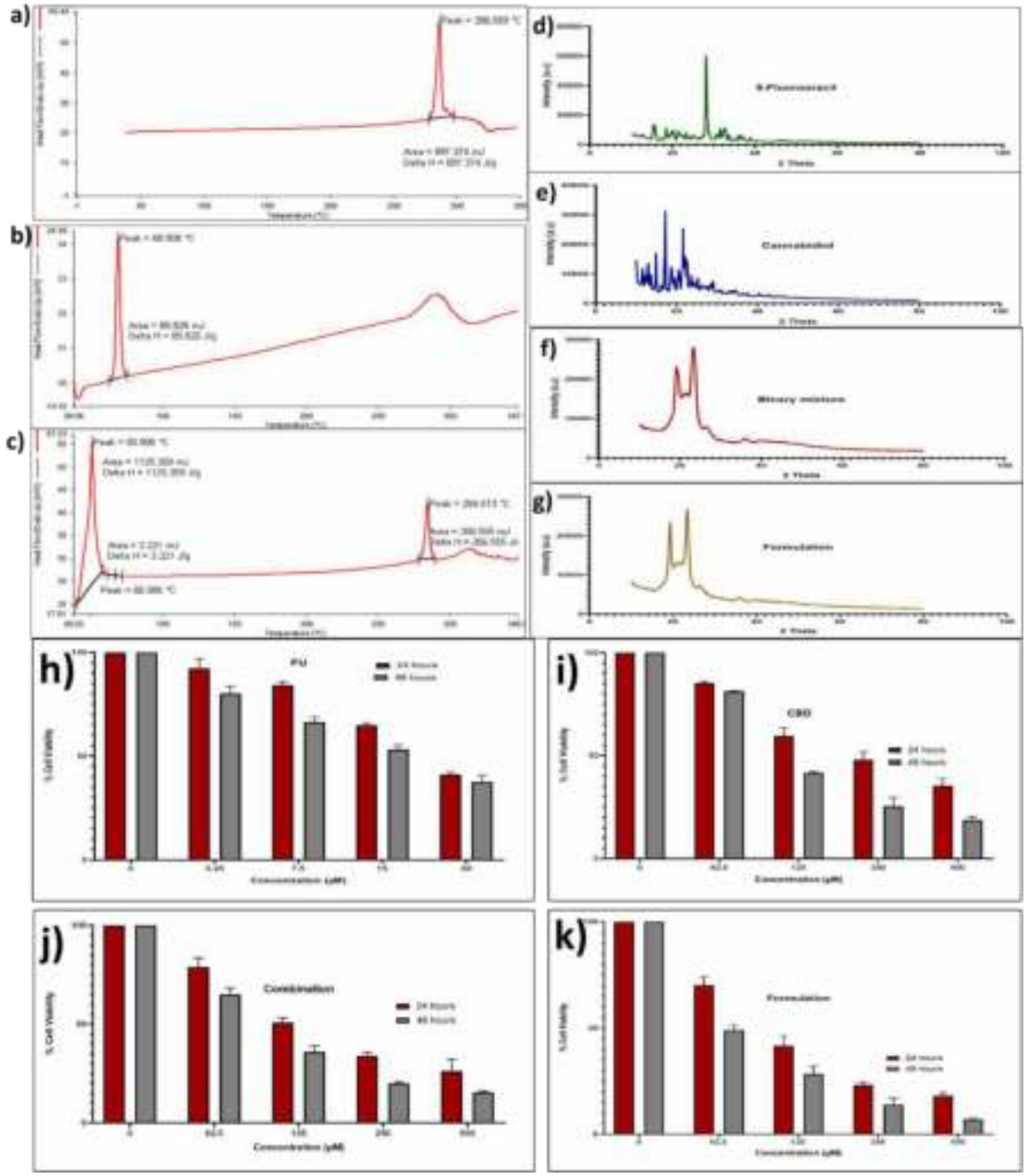

Figure 9: a, b and c represent DSC graphs of 5-FU, CBD and FU-CBD-NLCs respectively. While figure d, e, f, g were graphical representation of XRD spectra of 5-FU, CBD, Binary mixture and FU-CBD-NLCs respectively. Percent cell viability of A431 cells treated with h),5-FU i), CBD j) Combination (FU-CBD), and k) Optimized FU-CBD-NLCs formulation have been demonstrated.

30.2 Wound healing assay

Wound healing or scratch test is affordable and easy to perform assay which explains the proliferation and migration ability of the cells. Cancer becomes more devastating when it reaches the nearby tissue. Such a migration if stopped at the initial level could extend the

survival rate of the neoplastic patients. The Figure 10a-i shows the migration and proliferation cells at 0h, 24h, and 36h. The area of wound closure is found to be maximum in those cells considered as control as no treatment was given in this group due to which cells migrated across the scratch edges just like the cancer cells migrate in vivo. However, the least closure was observed on cells treated with NLC-FU-CBD which was significantly lower than those treated with 5-FU only. This is due to the synergistic effect of CBD with 5-FU as CBD in combination could successfully inhibit in vitro cell invasion and migration. The antiproliferative effect of these treatments is also due to the employment of NLC through enhanced permeation as compared to plain anti-cancer agents [13].

30.3 Nuclear morphology Assessment (DAPI staining Test)

DAPI dye stains the dsDNA in A-T rich region. The cells stained with DAPI dye were analyzed at 461nm). As demonstrated in Figure 10j-l, the cells of the control group showed normal nuclei, however, cells treated with NLC-FU-CBD showed more shrinkage, apoptosis, and fragmented nuclear morphology than FU-CBD. A comparative result of NLC-FU-CBD with FU-CBD is due to slow release, higher internalization, and greater accumulation of NLC into the cells which the conventional preparation failed to deliver. From the results, it was evaluated that NLC-FU-CBD could be a potential candidate for amelioration the skin carcinoma.

30.4 Cell Cycle Analysis

The cell cycle is responsible for cellular proliferation that bring cell division. Unbalanced regulation of the cell cycle results in abnormal cell division which may lead to cancer. Several therapeutic agents act by inducing cell cycle arrest at G0/G1, S, or G2/M phases of the cell cycle. In the present study, it is confirmed that, both conventional as well as prepared FU-CBD-NLCs exhibit the cell cycle arrest at G0/G1 phase of the cell cycle FU-CBD-NLCs caused a higher percentage of cell arrest (81.8%) in the G0/G1 phase of the cell cycle as compared to conventional (75.7%) in A431 cell line. Higher efficacy could be attributed due to the synergetic effect of 5-FU and CBD (shown in Figure 10m-o). Additionally, the nanonized form leads to better permeation of drugs into cells which improves the therapeutic efficacy. Thus, a prepared formulation could be a better alternative to conventional formulation in combating skin cancer [23].

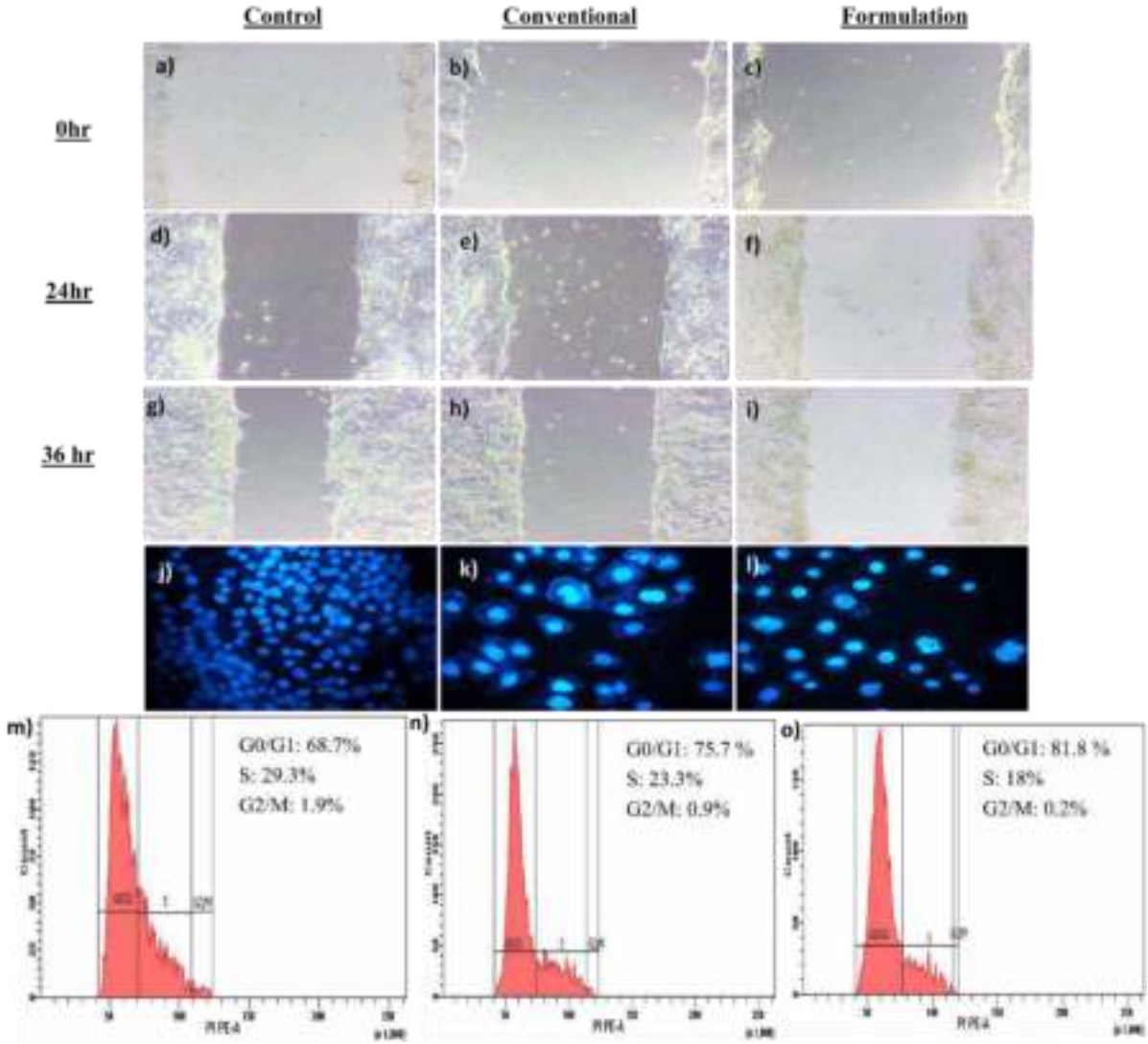

Figure 10: In Vitro wound healing assay: Inhibition of cell migration potential observed at 0, 24, and 36 hours of control (figure a, d and g), conventional (b, e, and h) and FU-CBD-NLCs Formulation (c, f, and g). Figure j, k and l represents DAPI staining analysis of control, conventional formulation and FU-CBD-NLCs Formulation. Cell cycle analysis of control cells, cells treated with conventional formulation and FU-CBD-NLCs formulation represented in figure m, n and o respectively.

31. Formulation of FU-CBD loaded NLC gel and its evaluation

FU-CBD-NLCs gel was prepared by using 1% Carbopol 934 as it contains good cohesive characteristics, and has easy wash-off nature. The prepared gel was evaluated based on pH, physical examination, and homogeneity. Later, Content Uniformity, Extrudability, and Spreadability followed by Rheological Studies and texture profile analysis of prepared FU-CBD-NLCs gel were analyzed.

31.1 Physical examination and pH evaluation

The prepared FU-CBD-NLCs gel was smooth in texture, whitish in color, and homogenous and no cracking and phase separation was observed. The pH of FU-CBD-NLCs gel was found 6.42 ± 0.037 at the temperature of 25 ± 1ºC. obtained pH suggests that the prepared gel was acceptable for dermal application. Furthermore, homogenous color, and texture, with no phase separation and no cracking in prepared FU-CBD-NLCs gel reveals that the prepared gel was stable and suitable for use[76].

31.2 Content Uniformity, Extrudability, and Spreadability

The Content uniformity of FU-CBD-NLCs gel was discovered to be 98.18 ± 1.23 %. Result obtained in content uniformity suggests that FU-CBD-NLCs were well distributed in the gel base and every portion of gel possesses an equal amount of FU-CBD-NLCs as well as a uniform amount of drug. The extrudability of the FU-CBD-NLCs gel was found to be 173.48 ± 0.438g. obtained extrudability value suggests that prepared gel will be easily extrudable from the tube. Further, the Spreadability of the FU-CBD-NLCs gel was found to be 7.06 ± 0.015 gcm/s which indicates easy Spreadability. As Spreadability values suggest a remarkable role in patient compliance and aid in uniform application of gel over the skin. The prepared gel takes less time to spread and has a low Spreadability value. The low value of Spreadability indicates that by the small amount of shear, gel was easily spread and also possessed acceptable bio-adhesion. Thus, the overall result of gel evaluation reveals that prepared FU-CBD-NLCs gel possesses an acceptable range of Content Uniformity, Extrudability, and Spreadability thus, the formulation could be carried out for further analysis. The obtained result was in accordance to our previously published paper [61].

31.3 Rheological Studies: viscosity measurement

The rheological characteristics of FU-CBD-NLCs gel were determined. Firstly, the flow behavior of FU-CBD-NLCs was demonstrated through a rheogram. These rheograms shows the values of shear stress and viscosity obtained at different shear rates which have been depicted in Figure 11a. The figure reveals the change in viscosity of gel upon changing the shear rate. The obtained rheogram indicates the shear-thinning behavior of prepared optimized FU-CBD-NLCs gel formulation which is similar to already published results [42]**.** Under amplitude sweep condition, the graph plotted between G', G" at Y-axis and strain at X-axis, it was found almost linear which can be observed in Figure 11b. which disclosed quite high storage modulus (G') as compared to loss modulus (G") which further authinticate the high elasticity of gel that retains virtue of less dissipation of energy, and loss in modulus would be high when the sample is predominantly viscous**.** It possible to determine the

internal alteration in the structure of the gel due to outcome of the frequency sweep study. The values for the storage modulus (G'), loss modulus (G''), and complex viscosity (η) were laid down across the frequency range. As depicted in Figure 11c, no cross-over was seen, while both storage and loss modulus were found to increase whereas linear reduction in complex viscosity was observed. This pattern delineates the higher efficiency of the sample (increase in modulus) with a decrease in measurement time (frequency = 1/time)[30]. The sample was also subjected to analysis for temperature sweep up to 50˚C temperature. There was no abnormal behavior observed at 25 ˚C. In brief, it can be easily transported if gel formulation has attained a particular phase and viscosity and stored at ambient temperature provided it is not subjected to any shear changes which might alter its viscosity and in turn stability and structure.

31.4 Texture profile analysis

The texture profile analysis of FU-CBD-NLCs gel was based on consistency, firmness, cohesiveness, and work of adhesion. At completion, the result, the force-time graph was obtained which is shown in the Figure 11d. The firmness of prepared gel was found to be 147 g force. Firmness is a descriptive term defined as the maximum force required to deform or fracture a product. The results of the prepared gel showed that FU-CBD-NLCs gel is resistant to deformation. Usually, high firmness leads to less spreading however our spreadability results showed that FU-CBD-NLCs gel is spreadable even being more resistant to deformation. The consistency of prepared FU-CBD-NLCs gel was found to be 259 g.sec. Consistency relates to the viscosity of the product and describes the texture and firmness of the product. According to the analysis, a high consistency value indicates that FU-CBD-NLCs gel was consistent. Cohesiveness is nothing but how well the product withstands a second deformation relative to its resistance under the first deformation. The maximum force represents sample adhesiveness or stickiness. The results of our studies indicate that FU-CBD-NLCs gel is more adhesive or sticky compared as it showed high cohesiveness (-116.74 g force) and work of cohesion -135.34 g.sec. Higher adhesion for FU-CBD-NLCs gel translates into higher contact time with skin which will lead to the possibly less frequent application of the gel. The obtained values for are in accordance to the published paper [61].

32. In-vitro release and Ex-vivo permeation study

As it is well-known fact that the target site for skin cancer is the epidermis and dermis. Thus, the prepared formulation should penetrate through the stratum corneum and should reach the dermis and epidermis layer of the skin. Additionally, the release of the drug to the site should be constant and slow to get prolonged action with minimal systemic absorption [5]. In *In-*

vitro permeation analysis cumulative amount of drug released for 5-FU was found to be 166.102 μg/cm^2 and 62.50 μg/cm^2 with flux values of 14.7 and 3.9 from FU-CBD-NLC gel and conventional gel respectively (shown in Figure 11e). While in the case of CBD cumulative amount of drug released was found to be 435.26 and 246.54 μg/cm^2 with flux values of 22.03 and 13.27 from FU-CBD-NLC gel and conventional gel respectively (shown in Figure 11f). In the case of ex vivo permeation analysis, the cumulative amount of 5-FU permeated was found to be 143 μg/cm^2 and 44.13 μg/cm^2 with a flux value of 12.07 and 3.95 from FU-CBD-NLC gel and conventional gel respectively (shown in Figure 11g). While in the case of CBD cumulative amount permeated was found to be 341.92 and 96.38 μg/cm^2 with flux values of 21.59 and 11.82 from FU-CBD-NLC gel and conventional gel respectively (shown in Figure 11h). The obtained result suggests that CBD, as well as 5-FU, permeated in higher concentrations through stratum corneum from FU-CBD-NLCs gel. Improved permeation of CBD, as well as 5-FU, was due to nanonized size of the formulation as well as occlusive behavior of NLCs, occlusive behavior leads to the dilation of openings of intercorneocyte by hydration of skin and alteration of corneocytes which results in better deposition of the drug via FU-CBD-NLCs gel [5].

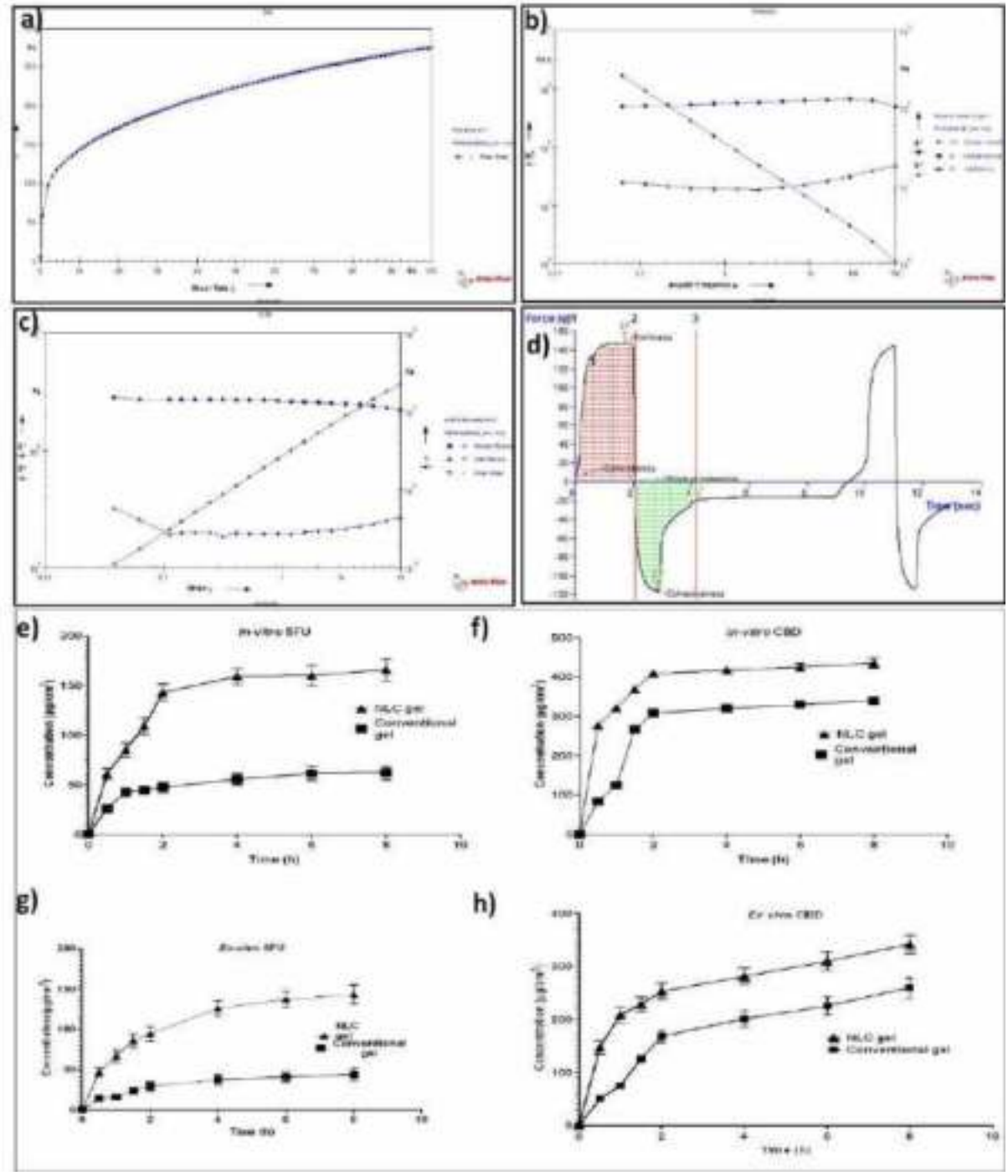

Figure 11: Illustration of rheological behavior of optimized FU-CBD-NLCs gel formulation a) Relationship between viscosity vs. shear rate b) Frequency sweep test, c) frequency sweep Test, and d) Shows Texture profile analysis of FU-CBD-NLCs gel. Figure e-h shows *In-vitro* and *Ex-vivo* profil©(e) Comparative *In-vitro* permeation study of 5-FU; (f) Comparative *In-vitro* permeation study of CBD; (g) Comparative permeation study of 5-FU through rat skin (h) Comparative permeation study of CBD through rat skin.

33. Dermatokinetics

The comparative drug deposition pattern in dermal layer and epidermal layer of FU-CBD-NLCs gel and the conventional gel was studied and illustrated in Figure 12a-12d. The non-compartmental analysis shows C_{max} of 5-FU from FU-CBD-NLCs gel was 100 and 137.39 $\mu g.cm^{-2}$ in the epidermal and dermal layers respectively which was much higher than the C_{max} of 5-FU from conventional gel i.e., 37.48 and 40.03 in epidermal and dermal layer respectively. The comparative parameters such as C_{max}, $T_{skin\text{-}max}$ (h), $AUC_{0\text{-}8hr}$ ($\mu g.cm^{-2}\ h^{-1}$) of 5-FU and CBD from conventional and FU-CBD-NLCs gel formulation were well tabulated in the Table 8. Higher value of Cmax and $AUC_{0\text{-}8hr}$ shows better penetration efficacy of the prepared FU-CBD-NLCs. The T_{max} value at each layer was significantly reduced in the case of FU-CBD-NLCs gel which is due to better permeation and rapid distribution of nanoformulations compared to the conventional formulation. Thus, the findings of the dermatokinetic study indicate that FU-CBD-NLCs gel crossed the skin barrier more efficiently and a higher concentration of the drug was delivered to the target site. Thus, it can be concluded that FU-CBD-NLCs gel leads to better permeation and accumulation of drugs into the epidermis layer and dermis layer of skin. This is probably due to the nanosized as well as the occlusive nature of this formulation which can improve the therapeutic efficacy.

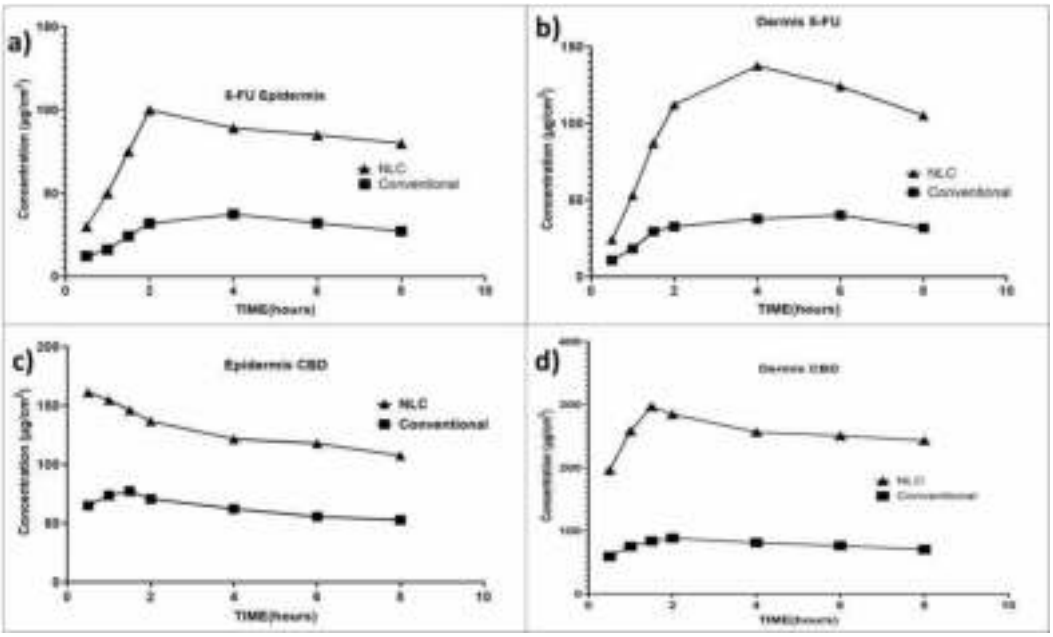

Figure 12: Comparative Graphical representation of amount of drug present in a) Epidermal 5-FU concentration profile (b) Dermal 5-FU concentration profile (c) Epidermal CBD concentration profile (d) Dermal CBD concentration profile. And release behavior through *in vitro & ex* vivo models.

Table 8: Comparative dermatokinetic parameters of conventional gel and FU-CBD-NLC gel

Comparative dermatokinetic parameters of conventional gel and FU-CBD-NLC gel								
Parameters	**Conventional Gel**				**FU-CBD-NLC gel**			
	5-FU		**CBD**		**5-FU**		**CBD**	
	Epidermis	**Dermis**	**Epidermis**	**Dermis**	**Epidermis**	**Dermis**	**Epidermis**	**Dermis**
$C_{skin\text{-}max}$ ($\mu g.cm^{-2}$)	37.48	40.03	77.26	88.57	100	137.39	161.16	296.92
$T_{skin\text{-}max}$ (h)	4	6	1.5	2	2	4	0.5	1.5
$AUC_{0\text{-}8hr}$ ($\mu g.cm^{-2}\,h^{-1}$)	232.69	256.95	484.45	605.36	630	849.79	987.88	1988.86

34. Formulation development and characterization

The FU-CBD-NLCs were successfully developed by multiple emulsification method. The prepared formulation was further exposed to characterization. The FU-CBD-NLCs showed a mean hydrodynamic diameter of 207.2 nm and PDI of 0.257, indicating its suitability for dermal drug delivery (Figure 13a). The encapsulation of 5-FU and CBD in the core of lipid assist in the epidermal and dermal delivery for better accumulation at the required site [5]. The permeation would also be enhanced by permeation of nanoparticles through the cyst of skin neoplastic cell. The zeta potential of the obtained NLCs was found to be -11.9 Mv which is due to the presence of surfactants, co-surfactant and lipids (Figure 13b). The negative zeta potential is required to maintain the stability without aggregating the nanoparticles. The results obtained by SEM and TEM indicates spherical sized particles with smooth surface in a size range of 200 nm indicating its efficiency in dermal drug delivery (Figure13c and d) [78]. The obtained results were in alignment of [79].

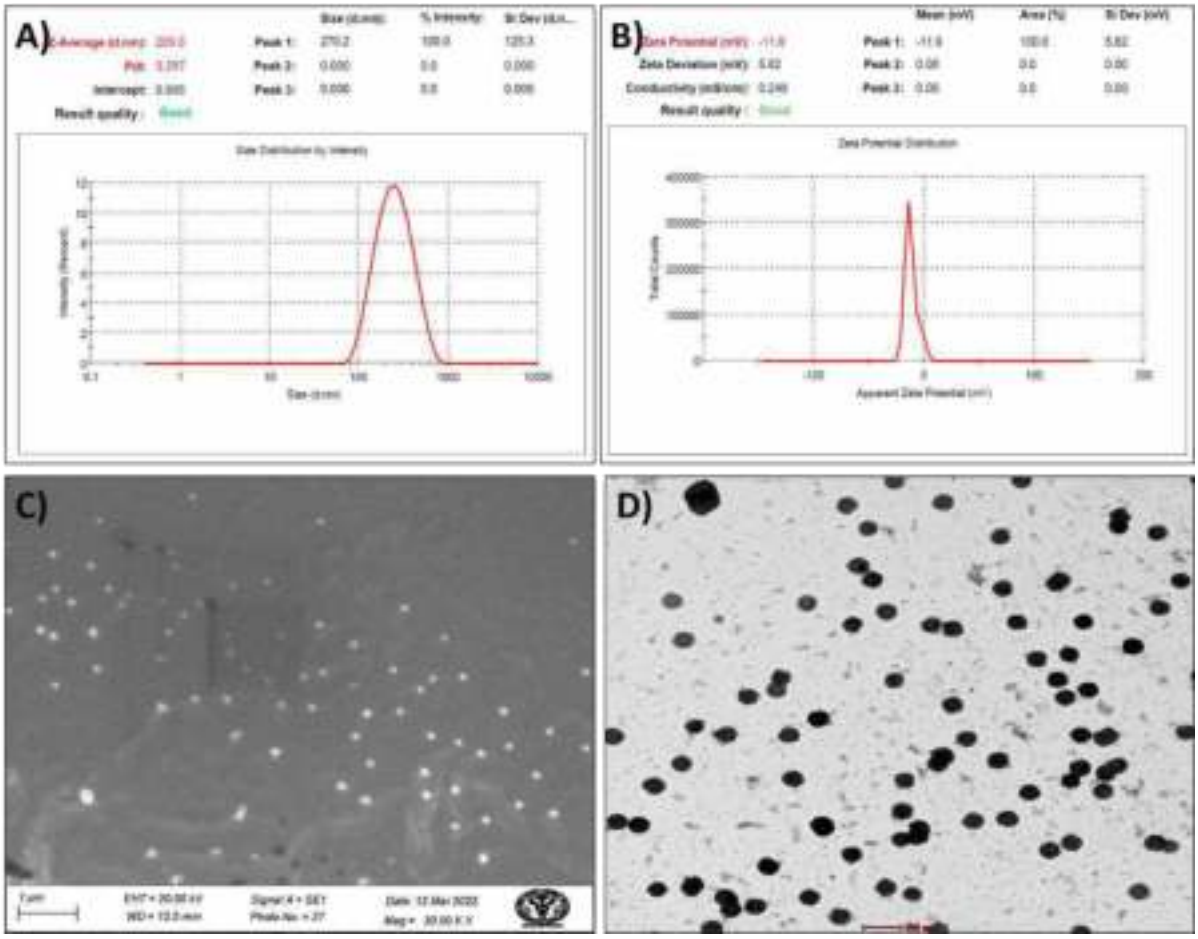

Fig. 13. Represents characterization of prepared FU-CBD-NLCs where figure a) shows zeta size and PDI analysis graph (b) shows zeta potential graph and micrographs for morphological examination of FU-CBD-NLCs- SEM and TEM were shown in figure c and d respectively.

35. Entrapment Efficiency

35.1 Formulation of FU-CBD loaded NLC gel and its evaluation

Carbopol-934 (1%) was selected to prepare FU-CBD-NLCs gel due to its excellent cohesive yet easy to wash-off characteristics. Once prepared, the FU-CBD-NLCs gel was evaluated for its physical appearance, homogeneity and pH. Further evaluation includes content uniformity assessment, extrudability Spreadability, along with texture analysis and rheological parameters assessment.

35.1.1 Physical examination and pH evaluation

The physical evaluation of FU-CBD-NLCs gel confirmed the smooth and homogenous texture of the gel and absence of any type of cracks or phase separation. This assured the stable nature of the prepared gel. The pH determined at 25 ± 1ºC temperature was found to be 6.52 ± 0.024 which is optimal for dermal application [76].

35.1.2 Content Uniformity, Extrudability, and Spreadability

The FU-CBD-NLCs loaded gel showed a Content uniformity of 98.37 ± 1.74 % indicating the well-distribution of NLCs particle in the gel matrix. Each portion of gel contains uniform amount of FU-CBD-NLCs and drug.

The Spreadability value of the FU-CBD-NLCs gel was 7.56 ± 0.018 g.cm/s, signifying easily spreadable nature of the gel. Spreadability of topical formulation plays a major role in patient compliance and benefit in uniform application of formulation over the dermal surface. The formulated NLC gel has low Spreadability value, which means that upon application of even little shear, gel will spread easily and will take less time to spread over the skin. Also, the gel showed acceptable bio-adhesion.

Furthermore, the extrudability of the FU-CBD-NLCs gel was 169.51 ± 0.348g indicating the optimum extrusion of gel from the tube upon application of certain weight.

Overall, the gel evaluation studies indicated that the formulated FU-CBD-NLCs gel has satisfactory range of Content Uniformity, Extrudability and Spreadability that it can be subjected to further analysis.

36. Skin irritation study

The applied site of conventional gel and NLC gel were investigated by measuring the temperature of the skin by infrared Camera. The temperature of the skin was recorded after 5 min, 0.5, 1, 2, 4, 8,12 hours of application of conventional gel and FU-CBD-NLCs gel. The comparison between the skin on which conventional gel and NLC gel was applied was performed after the application of respective gels over the skin of mice, to confirm whether the gels cause any irritation over the skin. The normal temperature range of mice skin i.e., 33°C–36°C is reported in the literature [80]. The maximum and minimum temperature of the applied site of the conventional gel were 37.4°C and 34.8°C respectively, whereas maximum and minimum temperature of applied site of NLC gel was 38.4°C and 35.2°C respectively. This mercurial range of temperature at conventional gel and NLC gel application site lucidly states that temperature falls within the normal temperature range of mice skin. Even though the recorded images (Figure 14a-g for conventional formulation whereas, Figure 14h to 14n for FU-CBD-NLCs gel at predetermined time intervals) delineate in a perspicuous manner about the temperature of conventional and NLC gel sites, which also validate the temperature reported in the literature for the mice skin. Thus, this comprehensive skin irritation study endorses that there was no skin redness and erythema observed during the study. Hence prepared formulation was as safe as conventional formulation.

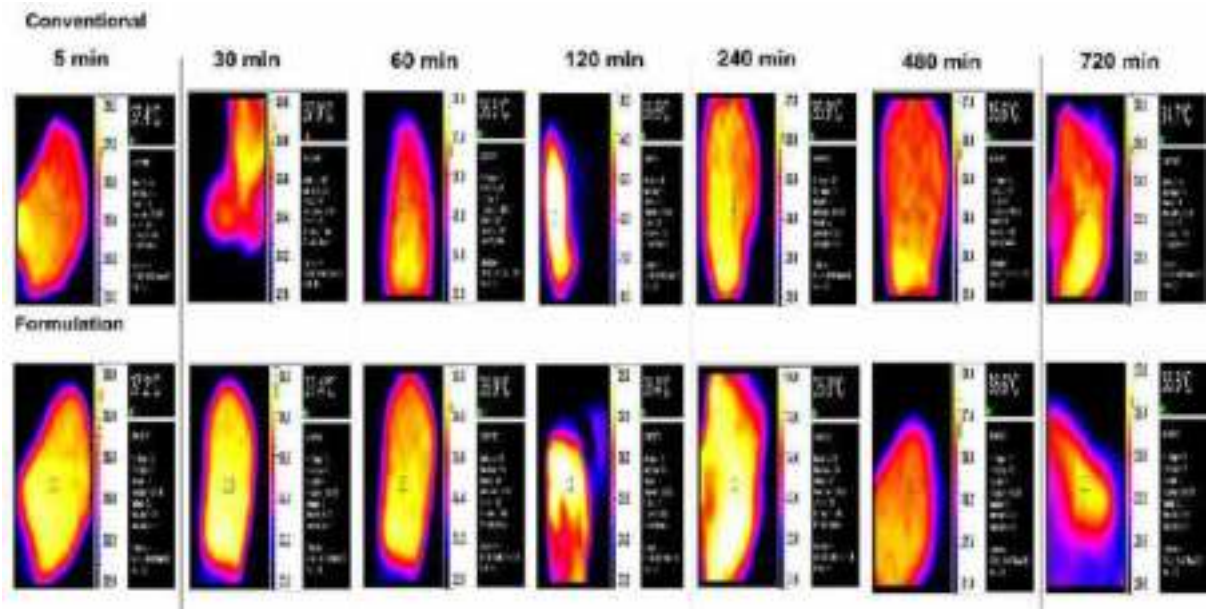

Figure 14: (a-g) represents thermographs of rat skin obtained at different time interval after application of conventional gel. (h-n) represents thermographs of rat skin obtained at different time interval after application of FU-CBD-NLCs gel.

37. Assessment of depth permeation of NLCs gel

The permeation of FU-CBD-NLCs from FU-CBD-NLCs gel through the skin was evaluated and compared using confocal laser scanning microscopy. Permeation of Rhodamine loaded conventional gel and rhodamine loaded-NLCs gel was evaluated and it was found that placebo gel shows less intensity of rhodamine in the skin layers with a mean intensity of 6.3 at 0 μm which gets reduced as the depth of the skin was increased as at 25 μm there was only 1.4 mean intensity which further reduces to 0.4 at 50 μm as can be observed in Figure 15a and b. While in the case of rhodamine loaded-NLCs gel prominent increase in intensity was observed in the skin layers and there was a sharp increase in the mean intensity. the mean intensity at depths of 0, 25, and 50 μm was found to be around 48 μm, 5 μm, and 1.4 μm as can be observed in the Figure 15c and d. Obtained results suggest that NLCs gel has the potential to deliver the drug. The better deposition of NLCs gel was attributed to its nano-size particles which enhance the permeation through the dermal layer. Nature, constituents, and occlusive effects of NLCs provide an edge to accumulate better in dermal layers. Thus, NLCs-gel could provide better accumulation with better therapeutic efficacy which will enhance the effect and will reduce the frequency of applying the gel.

38. Skin retention by Gamma Scintigraphy

38.1 Skin Retention analysis by Gamma Scintigraphy

Radiolabeling of 5-FU-CBD was accomplished by ^{99m} Technetium pertechnetate (^{99m}Tc) with the help of stannous chloride as a reducing agent. Several factors play important role in radiolabeling efficacy and those factors were optimized using QbD software. 13 combinations of stannous chloride and incubation time were given by the software and radiolabelling efficacy at each combination and radiolabelling efficacy as the response was observed and shown in the Table 9.

Table 9: Response analysis of dependent variables on different combination of independent variables for optimization of radiolabelling efficacy.

Runs	**Independent Variables**		**Dependent Variables**
	X_1= Stannous Chloride	X_2 = Incubation Time	Y_1 = Radiolabelling efficacy
1	2.5	0.413793	96.9
2	1	3	91.7
3	2	1	99.6
4	2	1	99.4
5	2	3.62132	99.5
6	0.37868	1.5	72.3
7	2	1	99.4
8	2	1	99.2
9	1	0.142857	72.6
10	4.62132	1.5	95.1
11	4	0	89.3
12	4	3	99.2
13	2	1	99.4

38.2 The effect of independent variables on radiolabeling efficacy.

Obtained Experimental data at each combination of the dependent variable was analyzed by the software and fitted in the quadratic model as it was proclaimed as the best-fitted model by software. The developed model was highly significant as the p-value was found to be $<$ 0.0001 by ANOVA analysis. The obtained model F-value of 386.90 indicates the applied model is significant. Additionally,68.69 value was obtained for Lack of Fit F-value which

indicates significant lack of fit as can be seen in figure 15e. The Predicted and adjusted R^2 was found to be 0.9529 and 0.9938 respectively. As the difference between so the applied model suggests reasonable adjustments. Model precision was analysed in terms of signal-to-noise ratio and it was found to be 53.157 indicates an adequate signal. As obtained ratio greater than 4 is desirable post analysis.

The obtained equation after analysis is shown as equation 6. and it suggests that stannous chloride (A), as well as Incubation time, has a positive effect on radiolabeling efficacy as radiolabeling increases with an increase of factors A and B but the saturation of radiolabeling efficacy was observed at 2mg/mL of stannous chloride solution and 1 hour of incubation time (Figure 15e). Thus, 2mg/mL of stannous chloride solution and 1 hour of incubation time were marked as the optimized range for best radiolabeling efficacy (99.6 %).

Radiolabeling efficacy = $+106.96+7.37A+7.84B -2.91AB-11.55A^2-7.99B^2$ ….*Equation 6*

38.3 Gamma scintigraphy investigation

Gamma scintigraphy studies were performed to determine localization, biodistribution, and skin uptake of prepared FU-CBD-NLCs from FU-CBD-NLCs gel. Optimized radiolabeled particles were added to the Carbopol gel base and then applied over the dorsal shaved skin of the rat. The acquired scintigraphy analysis reveals that FU-CBD-NLCs show prominent deposition on the skin once the gel was applied. Interestingly, maximum radioactivity was detected in the skin till 10 hours which indicates that NLCs will penetrate from the epidermis but get deposited into the skin layers without any ubiquitous dispersion of radioactivity to other organs as can be observed in scintigrams shown in the Figure 15f-l. The obtained result confirms and validates the CLSM results. Thus FU-CBD-NLCs demonstrate superior targeting ability to the skin additionally, radioactivity in plasma and blood was not detected during the complete study also radioactivity counts in major body organs such as the brain, kidneys, lungs, heart, liver, and spleen were found below the detection limit. For treatment of skin cancer, deeper skin layers were targeted and maximum concentration should be accumulated at the targeted site to reduce the systemic effect and side effects of the drug. There was no dissipation of the drug in the muscles at the site of application. Obtained scintigraphy results indicate that NLCs will greatly enhance the availability of the drugs in the skin layer and will reduce the side effects with improved therapeutic effects this could be due to the nature of NLCs as they are completely biodegradable with no or low toxicity. Their smaller size enables them to penetrate better in the skin layers and to have close contact with the skin [10], [11]. Obtained gamma scintigraphy results were in alignment of results obtained by [81]. Thus, FU-CBD-NLCs will greatly enhance the drug permeation into the

skin, also, it increases the skin hydration, minimize skin irritation, enhance the chemical stability of the drug, and thus improve the benefit/risk ratio.

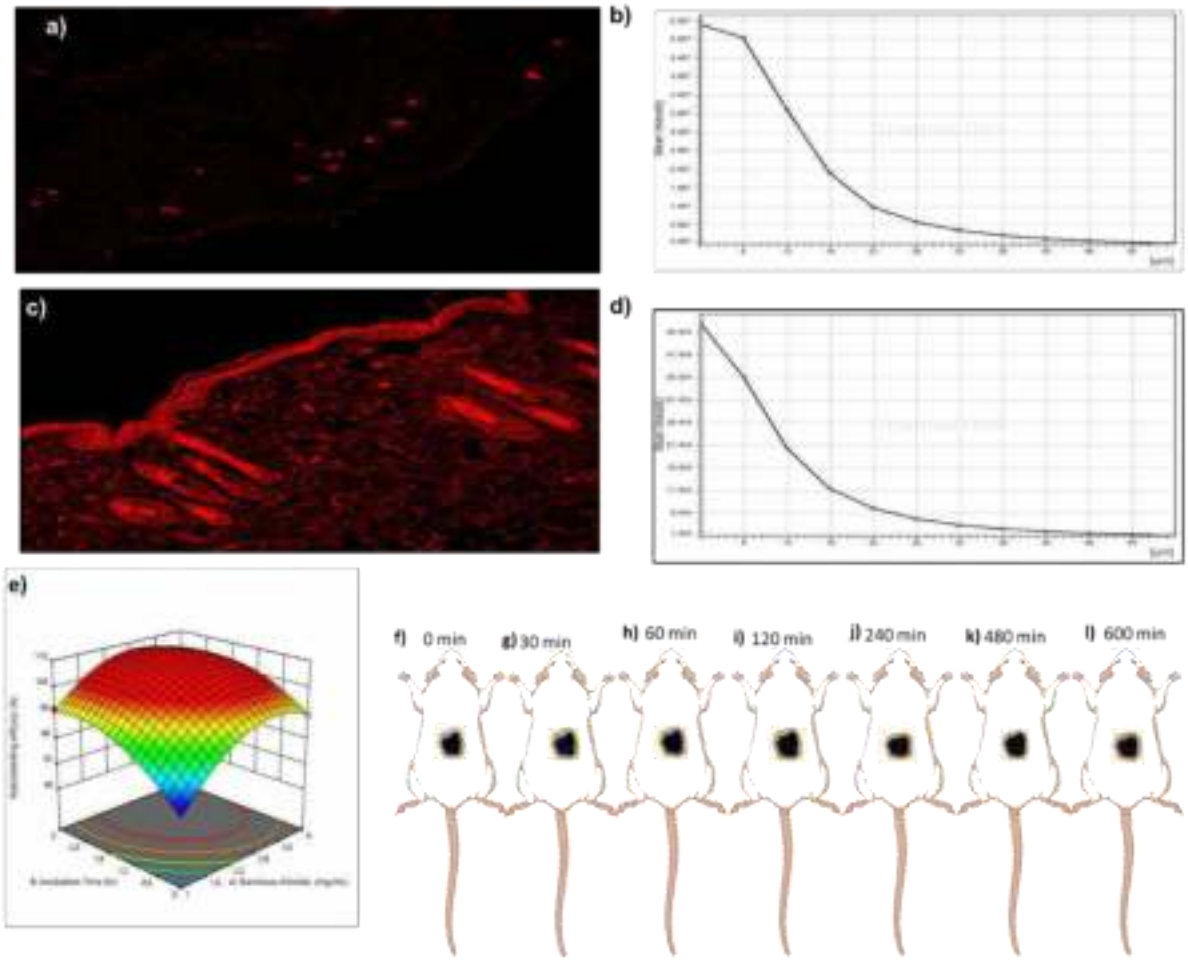

Figure 15: Depth analysis investigation by employing the confocal microscopy of a) conventional formulation, b) FU-CBD-NLCs with depth permeation graph of c) conventional formulation, and d) FU-CBD-NLCs gel. Representation of effect optimization of radiolabeling efficacy and effect of independent variable on dependent factors (e). e-l Represents accumulation and biodistribution behavior of FU-CBD-NLCs gel by gamma scintigraphic images captured after different interval of time.

39. In-Ovo Irritation studies

The comparative *In-Ovo* irritation studies of conventional formulation and FU-CBD-NLCs gel was conducted and the vascular response was observed and shown in the Figure 16a-h. When the conventional dose was administered no vascular response was observed till 2X of the dose. When 3X and 4X dose of the conventional dose was administered vascular response was observed as hyperemia and small areas of hemorrhage were observed and can be seen in the Figures 16e to h. After that, the formulation was administered and the vascular response was observed till the 4X dose as can be seen in the Figure 16a-d. The obtained result suggests that prepared FU-CBD-NLCs were much safer and more non-irritant compared to the

conventional gel which could result of encapsulation of the drug and matrix formation of drug and lipid in FU-CBD-NLCs. Matrix formation leads to a slow-release pattern of the drug from the FU-CBD-NLCs and thus prepared FU-CBD-NLCs systems were perceived as being suitable for in vivo use.

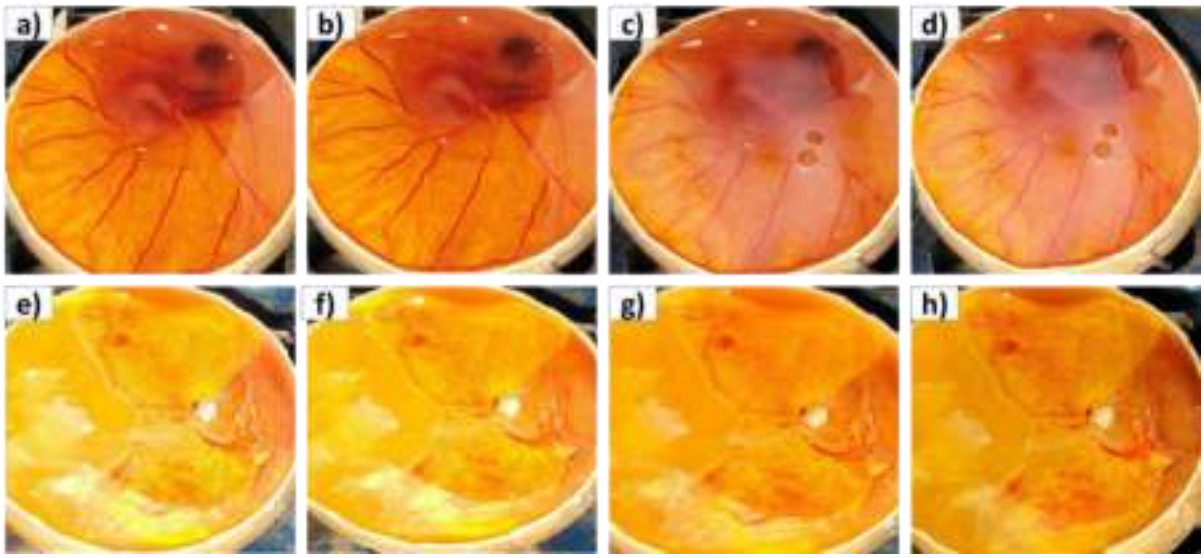

Figure 16: a-d shows HET-CAM analysis for prepared FU-CBD-NLCs Formulation whereas, Figure e to h represents HET-CAM irritation test for conventional drug solution.

40. In-Ovo Anti-tumor efficacy studies

The In-Ovo Anti-tumor studies have been used as a promising alternative to animal studies. The solid skin tumor was successfully grafted into the egg membrane with the help of skin cancer cell line A431 thus, the formed tumor will mimic the skin cancer. As can be depicted from the Figure 17a conventional formulation significantly reduces the tumor volume but FU-CBD-NLCs exhibit a higher inhibition rate. The higher tumor inhibition indicates that nanoformulations exhibit better penetration of 5-FU and CBD into the tumor environment. Thus, enhanced permeation of both drugs not only provides specific targeting, in addition but also improves the anti-cancer efficacy of the formulation. The obtained tumor mass was then processed for histological analysis. The histological analysis shows that tissues of positive control were lined by keratinized stratified squamous epithelium. Sub epithelium shows circumscribed lesion comprising of the nodular aggregate of atypical cells with irregular punched out spaces in between. Atypical cells have an indistinct cytoplasmic border, round to oval nucleus with coarse chromatin, and inconspicuous nucleoli as can be seen in the Figure 17b-e. As can be seen in the Figure 17e the conventional formulation prevents the formation of the tumor but FU-CBD-NLCs greatly inhibit the formulation of tumors which proves the efficacy of the prepared formulation and the improved efficacy

and preventive effect of the formulation.

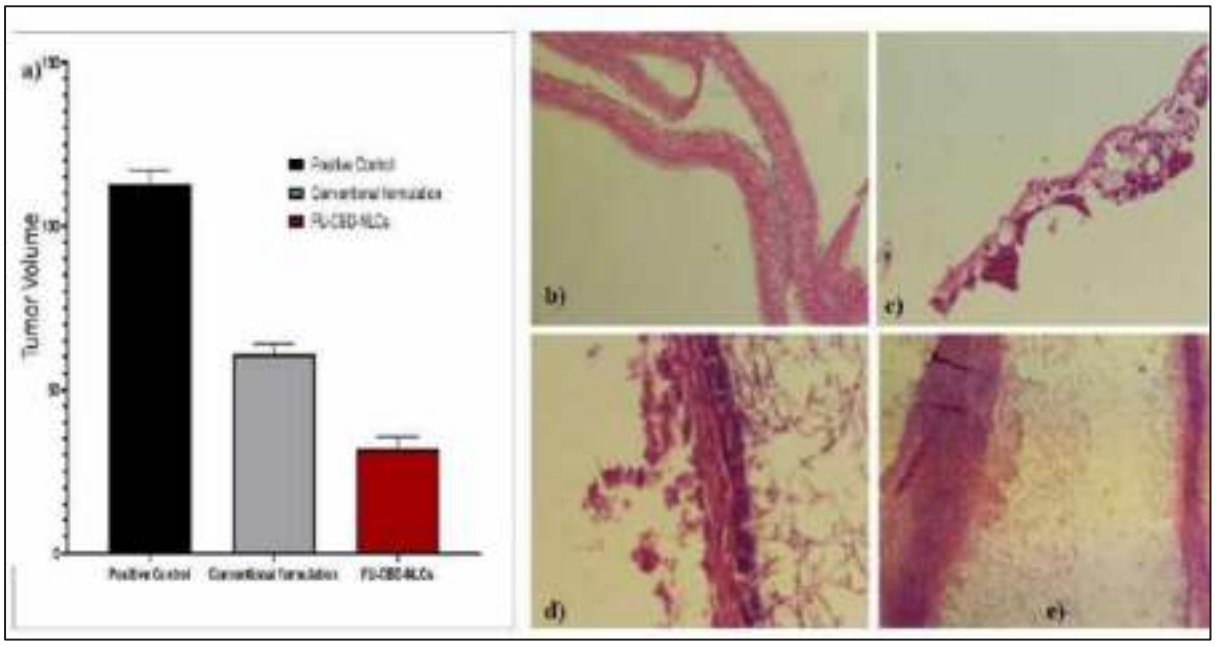

Figure 17: Comparative graphical representation of tumor weight in *In-Ovo* studies (a). Histopathology Photomicrograph of Tumor grafted egg membrane treated with b) Normal Saline (Control), c) no treatment (Positive control), d) Conventional formulation treated, e) FU-CBD-NLCs treated.

41. In-vivo tumor remission efficacy study.

After 14 weeks of tumor induction schedule when fully grown tumors of group III were treated with conventional formulation while group IV were treated with FU-CBD-NLCs-gel respectively. During 24 days of treatment, it was observed there was significant reduction in number of tumors of group IV compared to control and group III. On day 1 of the treatment rats of each group on average consists of 5 tumors but after 24 days of the treatment group II (positive control) group consists average 5 tumors per rat while in case of Group III average number of tumors got reduced to 3 comparative graphs shown in figure 18a. Rats treated with formulation i.e., Group IV shows 2 tumors on average which is attributed because of good penetration, retention and therapeutic efficacy of the prepared 5-FU-CBD-NLCs gel. Along with average number of tumors survivalists during the treatment was recorded and analyzed by survival graph plot shown in figure 18b. The survival graph plot shows the survival-ability of group IV was much higher when compared to the Group II (positive control) and Group III (conventional treatment). The survival-ability of group IV was around 70% while group II and III shows 26% and 50% survival only. The improved survival rate of the formulation treatment group signifies those prepared formulations shows better therapeutic efficacy with better survival rate. Additionally, Tumor area and volume were also measured during the

treatment schedule which were shown in figure 18c and d. On day 1 of the treatment schedule the average tumor area and volume of group II, III and IV was observed 44.88 ± 4.03, 46.76 ±1.02 and 46.33 ± 0.55 respectively. While on 24th day of treatment the tumor area and volume of group II, III and IV was observed 85.68 ± 1.44, 26.13 ± 0.51 and 13.87 ± 0.73 respectively. The observed tumor area and volume results shows that better reduction in tumor area and volume was observed in case of FU-CBD-NLCs formulation. The FU-CBD-NLCs gel was found twice therapeutic compared to conventional gel. All these notable therapeutic effects were due to nanosized nature of formulation, enhanced drug permeation, good occlusiveness behaviour, presence of cannabidiol in the formulation, and lipidic behaviour of formulation which all leads to better drug deposition at specific targeted site compared to conventional gel [61][9].

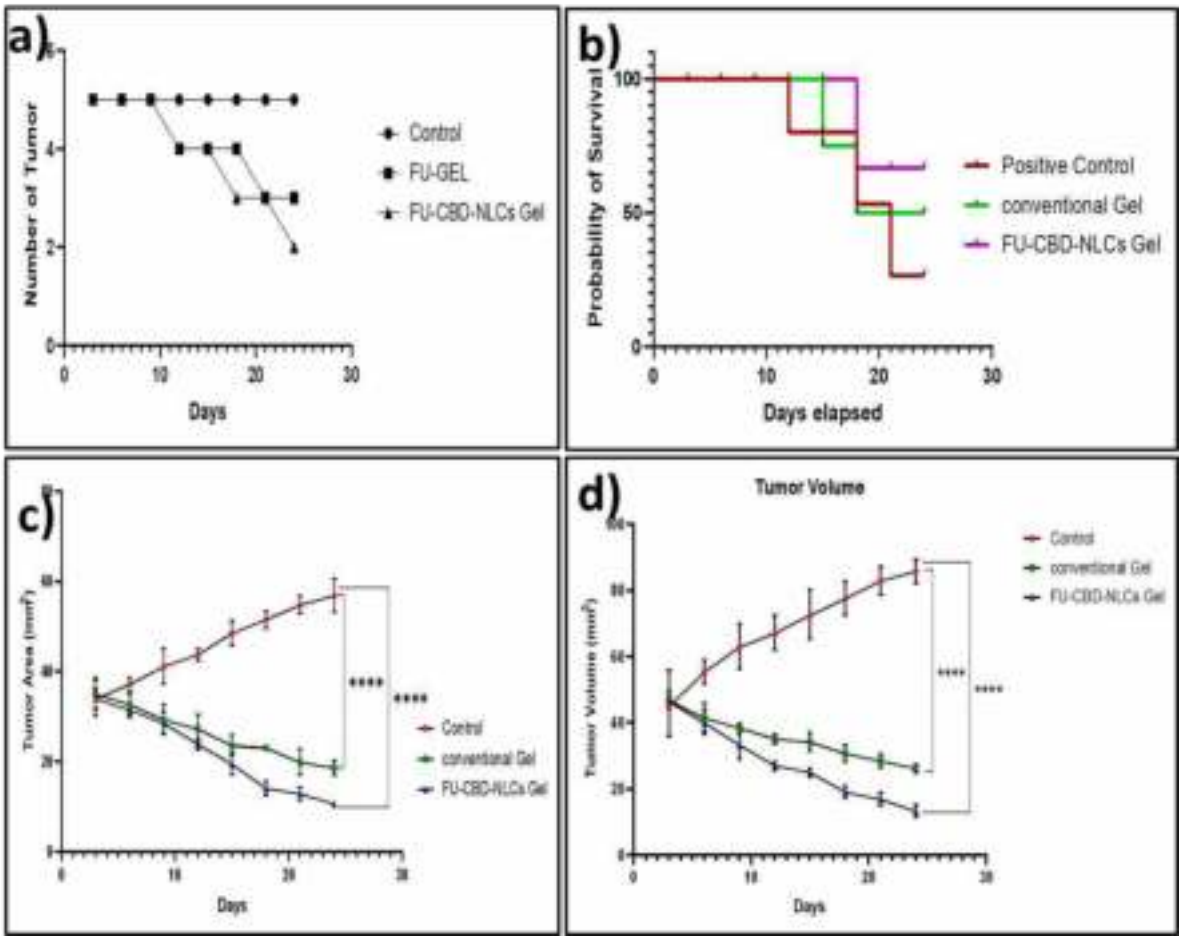

Figure 18: Tumor macro-analysis during treatment (a) changes in tumor number, (b) Probability of survival, (c) tumor area, and (d) tumor volume. ****p<0.0001 represent a reduction in tumor volume and area in animals in a significant manner.

42. Histopathological Analysis

Histopathological findings were standard for confirmation and diagnosis of different types of cancer. During the analysis of the slides of group I (normal control) it was found that the skin structure orientation was well defined the epidermal layer along with basal cells with dermal layer, hair shaft, and keratinocytes, with normal skin adnexa were clearly visible (Fig 19e). In case of positive control (group (II) hyperplasia very thick corneal layer was observed in the epidermal layer. clear invasion of epidermal layer was observed into the dermal layer. Additionally, there was clear presence of mitotic figures, keratin pearls, marked acanthosis, perineural invasion and hyperchromatic-megakaryocytic nucleus and downward elongation of rete ridges was observed and shown in figure 19f. Further, when slide prepared of skin samples of group III i.e., rats treated with conventional formulation was observed and shown in figure 19g. There was slight improvement in the histopathology of skin compared to group II. tumor tissues were found infiltrating into the sub epithelium but no intraepithelial keratin peral was observed. Lastly, when skin samples of tumors treated with FU-CBD-NLCs gel were observed and shown in figure 19h. It was found that the dermal and epidermal layers were clearly distinguishable. The absence of miotic figures and keratin pearls were present. Additionally, significant reduction in hyperchromatic-megakaryocytic nucleus was observed. Although, there was presence of mild structural damage and inflammatory cells in epidermal layer. Thus, overall finding of the histopathological analysis indicates FU-CBD-NLCs were more efficacious than conventional formulation which validates *In-vitro* cell line studies as well as *In-ovo* tumor remission studies along with *In-vivo* tumor remission study. The effectiveness of lipid-based nano system with presence of FU and CBD ameliorate the treatment of tumors [9]. Thus, results obtained were in alignment of [70] and histopathological analysis suggests and validates results of tumor analysis across whole analysis of the treatment paradigm.

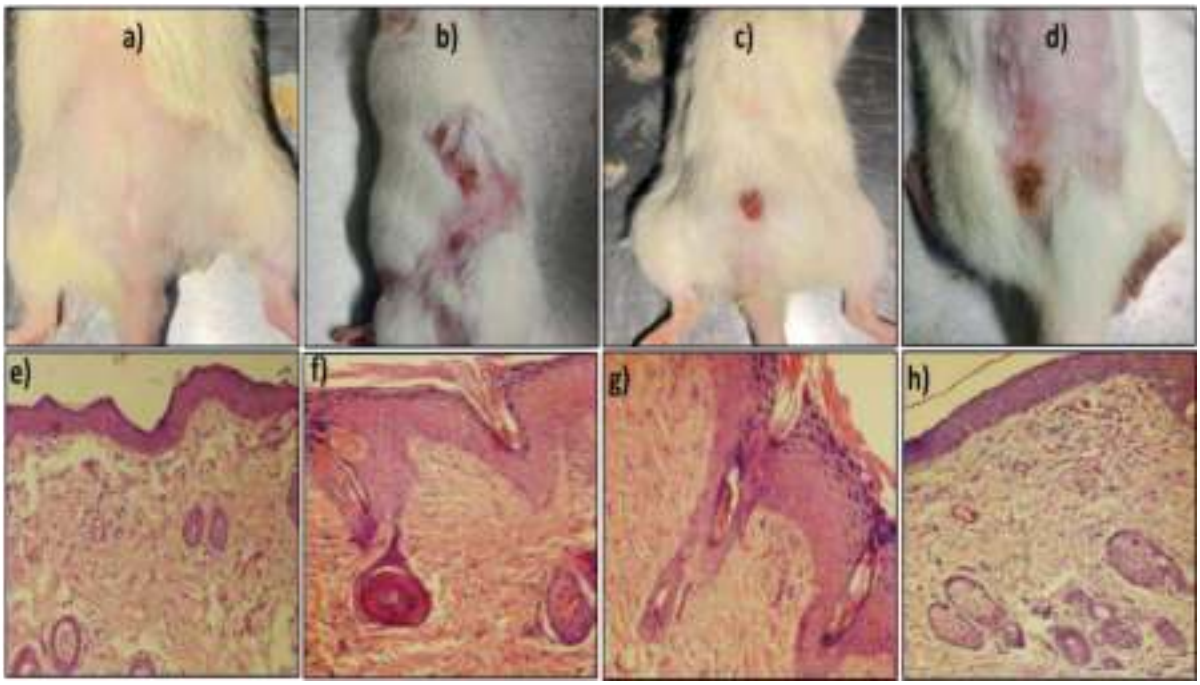

Figure 19: Comparative picture a) skin of normal control rat (group I), b) Tumor bearing rat without any treatment (group II), c) Conventional gel treated rat (group III), and d) FU-CBD-NLCs gel treated (group IV) while figure e, f, g and h shows their comparative photomicrograph of histopathology which shows prepared gel was more therapeutic than the conventional treatment.

43. Effect of combinatorial NLC-formulation on biochemical estimation

Biochemical estimation such as Malondialdehyde (MDA), catalase (CAT), glutathione (GSH) and Superoxide dismutase was determined by respective treatment to the respective groups, animals were sacrificed and then different tissues Skin. Effect of different treatment on the different biochemical markers. Catalase and GSH are the enzymes which facilitate quenching of free radical, superoxide and peroxide radicals thus higher-level offer defense against oxidative stress while reduced level of MDA indicates reduced lipid peroxidation [82]. Animals untreated and unexposed to DMBA demonstrated significantly high GSH and Catalase level value i.e., 49.59 ± 2.8 µg/mg of protein and 6.9 nmol H_2O_2 consumed/min/mg protein respectively. while significantly low Malondialdehyde level i.e., 6.17 ± 0.65 nmol/mg of protein was observed when compared with other groups.

Conventional formulation treatment group demonstrated significantly low GSH, CAT and SOD followed by high MDA level i.e., 26.31 ± 1.18 µg/mg of protein, 2.7 ± 0.55 nmol H_2O_2 consumed/min/mg protein, 9.4 ± 0.83 and 20.04 ± 1.8 nmol/mg of protein respectively.

Animals treated with FU-CBD-NLCs Gel demonstrates GSH, CAT, SOD and MDA level as 39.35 ± 0.67 µg/mg of protein, 3.94 ± 0.27 nmol H_2O_2 consumed/min/mg protein, 13.50 ± 0.99 and 12.49 nmol/mg of protein respectively which can be observed in figure 20a-d.

Obtained result were in alignment of [70] and confirmed that the homeostatic imbalance of endogenous enzymes caused by tumor was restored by conventional and FU-CBD-NLCs Gel. FU-CBD-NLCs Gel prevents oxidative stress which damage vital macromolecules like lipid, proteins and DNA better than conventional formulation this could be attributed due to presence of cannabidiol in the formulation and occlusive and retentive behavior of formulation. The finding supports that FU-CBD-NLCs Gel successfully ameliorated the enzyme balance and therefore promises to be a potential tool for antioxidant therapy and validates the previous studies.

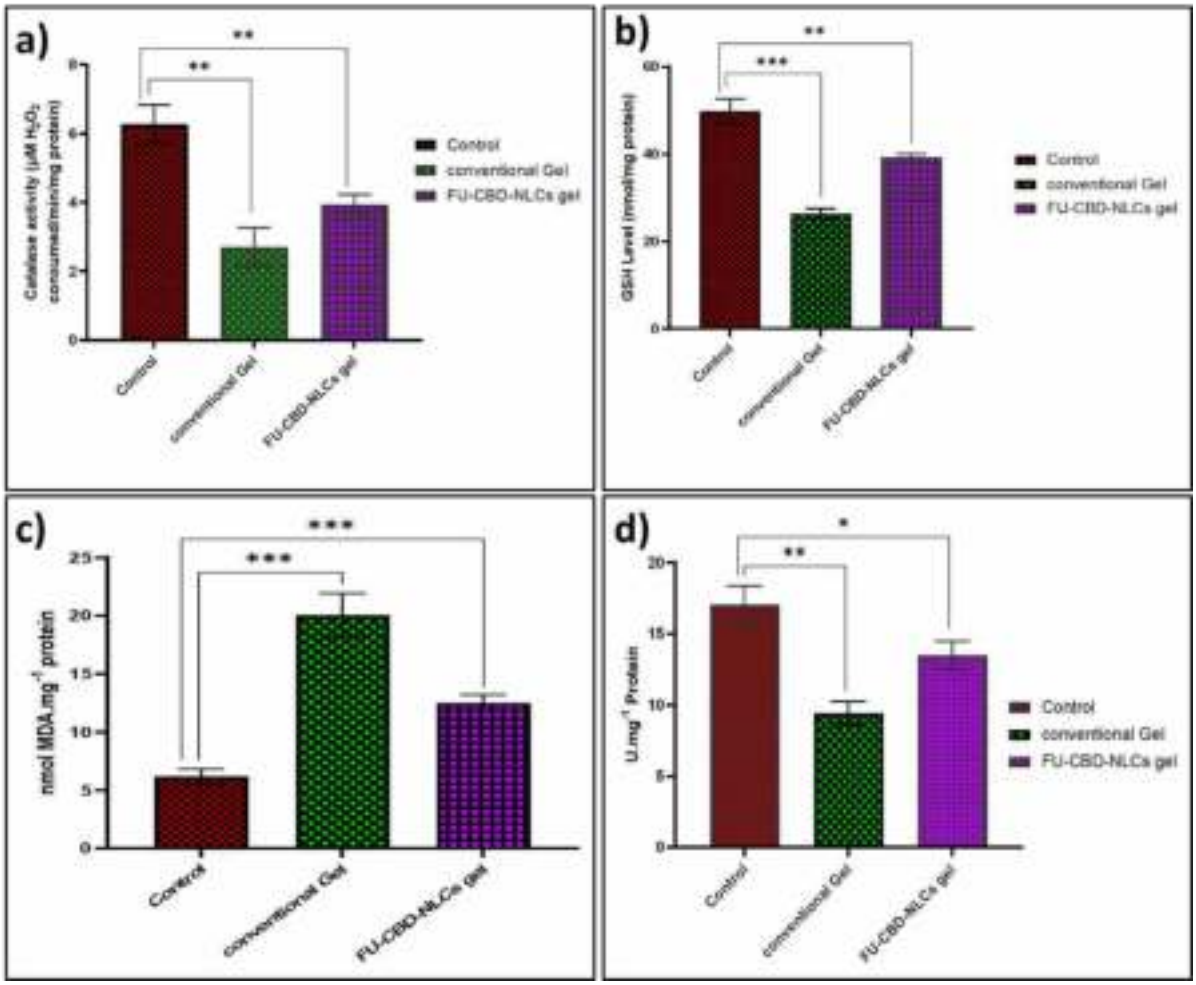

Figure 20: Effect of FU-CBD-NLCs gel and conventional gel on the marker of oxidative stress in the tumor induced SC tissue. (a) CAT (b) GSH (c) MDA and (d) SOD. Values were expressed as mean ± SD, followed by One-Way ANOVA Tukey's multiple comparison tests for statistical analysis.; *$p<0.05$, **$p<0.01$, ***$p<0.001$ represents significance treatment groups versus control group.

Impact of the research in the advancement of knowledge or benefit to mankind

The prepared formulation in the project was one of its kind and novel. The formulation was able treats the skin cancer more efficiently than conventional one thus this could be an alternative for the ongoing conventional therapy. Thus, research is a step ahead for better treatment of the skin cancer.

References

[1] X. Sun, N. Zhang, C. Yin, B. Zhu, and X. Li, "Ultraviolet Radiation and Melanomagenesis: From Mechanism to Immunotherapy," *Front. Oncol.*, vol. 10, p. 951, Jul. 2020, doi: 10.3389/FONC.2020.00951/BIBTEX.

[2] Y. Mohammed *et al.*, "Advances and future perspectives in epithelial drug delivery," *Adv. Drug Deliv. Rev.*, vol. 186, p. 114293, Jul. 2022, doi: 10.1016/J.ADDR.2022.114293.

[3] M. Neagu, C. Constantin, C. Caruntu, C. Dumitru, M. Surcel, and S. Zurac, "Inflammation: A key process in skin tumorigenesis," *Oncol. Lett.*, vol. 17, no. 5, p. 4068, May 2019, doi: 10.3892/OL.2018.9735.

[4] M. Imran *et al.*, "Overcoming Multidrug Resistance of Antibiotics via Nanodelivery Systems," *Pharm. 2022, Vol. 14, Page 586*, vol. 14, no. 3, p. 586, Mar. 2022, doi: 10.3390/PHARMACEUTICS14030586.

[5] M. K. Iqubal *et al.*, "Combinatorial lipid-nanosystem for dermal delivery of 5-fluorouracil and resveratrol against skin cancer: Delineation of improved dermatokinetics and epidermal drug deposition enhancement analysis," *Eur. J. Pharm. Biopharm.*, vol. 163, no. December 2020, pp. 223–239, 2021, doi: 10.1016/j.ejpb.2021.04.007.

[6] B. Hinz and R. Ramer, "Cannabinoids as anticancer drugs: current status of preclinical research," *Br. J. Cancer*, 2022, doi: 10.1038/S41416-022-01727-4.

[7] N. Hasan *et al.*, "Rapid analytical method development and validation for the simultaneous estimation of 5-Fluorouracil and Cannabidiol in plasma and lipid-based nanoformulations," *Curr. Anal. Chem.*, vol. 18, Mar. 2022, doi: 10.2174/1573411018666220304085236.

[8] M. Imran, K. R. Paudel, A. Insaf, N. Hasan, V. V Sugandhi, and D. Shrestha, "Unravelling the chemopreventive potential of antioxidants against various cancers," pp. 1–19, 2022.

[9] N. Hasan *et al.*, "Cannabis as a potential compound against various malignancies, legal

aspects, advancement by exploiting nanotechnology and clinical trials," *https://doi.org/10.1080/1061186X.2022.2056188*, pp. 1–17, Mar. 2022, doi: 10.1080/1061186X.2022.2056188.

[10] R. H. Müller, R. D. Petersen, A. Hommoss, and J. Pardeike, "Nanostructured lipid carriers (NLC) in cosmetic dermal products," *Advanced Drug Delivery Reviews*. 2007, doi: 10.1016/j.addr.2007.04.012.

[11] J. Pardeike, A. Hommoss, and R. H. Müller, "Lipid nanoparticles (SLN, NLC) in cosmetic and pharmaceutical dermal products," *International Journal of Pharmaceutics*. 2009, doi: 10.1016/j.ijpharm.2008.10.003.

[12] M. Imran, M. Kashif, K. Imtiyaz, and S. Saleem, "Topical nanostructured lipid carrier gel of quercetin and resveratrol : Formulation , optimization , in vitro and ex vivo study for the treatment of skin cancer," *Int. J. Pharm.*, vol. 587, no. July, p. 119705, 2020, doi: 10.1016/j.ijpharm.2020.119705.

[13] M. Haider, S. M. Abdin, L. Kamal, and G. Orive, "Nanostructured Lipid Carriers for Delivery of Chemotherapeutics: A Review," *Pharmaceutics*, vol. 12, no. 3, Mar. 2020, doi: 10.3390/PHARMACEUTICS12030288.

[14] R. Karwasra *et al.*, "Engineering macrophage targeted punicalagin nanoparticles by computational modeling to alleviate methotrexate induced neutropenia," Mar. 2022, doi: 10.21203/RS.3.RS-1441489/V1.

[15] B. Iqbal, J. Ali, and S. Baboota, *Silymarin loaded nanostructured lipid carrier: From design and dermatokinetic study to mechanistic analysis of epidermal drug deposition enhancement*, vol. 255. Elsevier B.V, 2018.

[16] N. Hasan *et al.*, "Intranasal delivery of Naloxone-loaded solid lipid nanoparticles as a promising simple and non-invasive approach for the management of opioid overdose," *Int. J. Pharm.*, vol. 599, no. January, 2021, doi: 10.1016/j.ijpharm.2021.120428.

[17] M. Alam, S. Zameer, A. K. Najmi, F. J. Ahmad, S. S. Imam, and M. Akhtar, "Thymoquinone Loaded Solid Lipid Nanoparticles Demonstrated Antidepressant-Like Activity in Rats via Indoleamine 2, 3- Dioxygenase Pathway," *Drug Res. (Stuttg).*, 2020, doi: 10.1055/a-1131-7793.

[18] P. Jagtap, K. Jadhav, and N. Dand, "Formulation and ex vivo evaluation of solid lipid nanoparticles (SLNS) based hydrogel for intranasal drug delivery," *Int. J. Medical, Heal. Biomed. Bioeng. Pharm. Eng.*, vol. 9, no. 1, pp. 43–53, 2015.

[19] A. S. Joshi, H. S. Patel, V. S. Belgamwar, A. Agrawal, and A. R. Tekade, "Solid lipid nanoparticles of ondansetron HCl for intranasal delivery: Development, optimization

and evaluation," *J. Mater. Sci. Mater. Med.*, vol. 23, no. 9, pp. 2163–2175, 2012, doi: 10.1007/s10856-012-4702-7.

[20] Ameeduzzafar, J. Ali, A. Bhatnagar, N. Kumar, and A. Ali, "Chitosan nanoparticles amplify the ocular hypotensive effect of cateolol in rabbits," *Int. J. Biol. Macromol.*, vol. 65, pp. 479–491, Apr. 2014, doi: 10.1016/J.IJBIOMAC.2014.02.002.

[21] D. Z. Hou, C. S. Xie, K. J. Huang, and C. H. Zhu, "The production and characteristics of solid lipid nanoparticles (SLNs)," *Biomaterials*, 2003, doi: 10.1016/S0142-9612(02)00578-1.

[22] K. A. Scott, A. G. Dalgleish, and W. M. Liu, "The combination of cannabidiol and Δ9-tetrahydrocannabinol enhances the anticancer effects of radiation in an orthotopic murine glioma model," *Mol. Cancer Ther.*, vol. 13, no. 12, pp. 2955–2967, Dec. 2014, doi: 10.1158/1535-7163.MCT-14-0402.

[23] B. Zeya, S. Nafees, K. Imtiyaz, L. Uroog, K. U. Fakhri, and M. M. A. Rizvi, "Diosmin in combination with naringenin enhances apoptosis in colon cancer cells," *Oncol. Rep.*, vol. 47, no. 1, 2022, doi: 10.3892/or.2021.8215.

[24] M. Imran *et al.*, "Topical nanostructured lipid carrier gel of quercetin and resveratrol: Formulation, optimization, in vitro and ex vivo study for the treatment of skin cancer," *Int. J. Pharm.*, vol. 587, p. 119705, Sep. 2020, doi: 10.1016/J.IJPHARM.2020.119705.

[25] V. Dave, N. Bhardwaj, N. Gupta, and K. Tak, "Herbal ethosomal gel containing luliconazole for productive relevance in the field of biomedicine," *3 Biotech*, vol. 10, no. 3, pp. 1–15, 2020, doi: 10.1007/s13205-020-2083-z.

[26] E. Sana *et al.*, "Topical delivery of curcumin-loaded transfersomes gel ameliorated rheumatoid arthritis by inhibiting NF-κβ pathway," *Nanomedicine*, vol. 16, no. 10, pp. 819–837, Apr. 2021, doi: 10.2217/nnm-2020-0316.

[27] A. Zakkula, B. B. Gabani, R. K. Jairam, V. Kiran, U. Todmal, and R. Mullangi, "Preparation and optimization of nilotinib self-micro-emulsifying drug delivery systems to enhance oral bioavailability," *Drug Dev. Ind. Pharm.*, vol. 46, no. 3, pp. 498–504, 2020, doi: 10.1080/03639045.2020.1730398.

[28] U. A. Khan *et al.*, "Parenteral sustained release lipid phase-transition system of ziprasidone: Fabrication and evaluation for schizophrenia therapy," *Drug Des. Devel. Ther.*, 2020, doi: 10.2147/DDDT.S247196.

[29] S. Jain, N. Patel, P. Madan, and S. Lin, "Formulation and rheological evaluation of ethosome-loaded carbopol hydrogel for transdermal application," *Drug Dev. Ind. Pharm.*, vol. 42, no. 8, pp. 1315–1324, 2016, doi: 10.3109/03639045.2015.1132227.

[30] A. K. Jain *et al.*, “Adapalene loaded solid lipid nanoparticles gel: An effective approach for acne treatment,” *Colloids Surfaces B Biointerfaces*, vol. 121, pp. 222–229, 2014, doi: 10.1016/j.colsurfb.2014.05.041.

[31] T. Coviello *et al.*, “Gel-embedded niosomes: Preparation, characterization and release studies of a new system for topical drug delivery,” *Colloids Surfaces B Biointerfaces*, vol. 125, pp. 291–299, 2015, doi: 10.1016/j.colsurfb.2014.10.060.

[32] P. I. Brånemark *et al.*, “Osseointegrated implants in the treatment of the edentulous jaw. Experience from a 10-year period.,” *Scand. J. Plast. Reconstr. Surg. Suppl.*, 1977.

[33] M. V Chandra and B. A. Shamasundar, “Texture Profile Analysis and Functional Properties of Gelatin from the Skin of Three Species of Fresh Water Fish,” *Int. J. Food Prop.*, vol. 18, no. 3, pp. 572–584, 2015, doi: 10.1080/10942912.2013.845787.

[34] A. Gull, S. Ahmed, F. J. Ahmad, U. Nagaich, and A. Chandra, “Hydrogel thickened microemulsion; a local cargo for the co- delivery of cinnamaldehyde and berberine to treat acne vulgaris,” *J. Drug Deliv. Sci. Technol.*, 2020, doi: 10.1016/j.jddst.2020.101835.

[35] S. S. Chavan, S. G. Ingle, and P. R. Vavia, “Preparation and characterization of solid lipid nanoparticle-based nasal spray of budesonide,” *Drug Deliv. Transl. Res.*, vol. 3, no. 5, pp. 402–408, 2013, doi: 10.1007/s13346-012-0105-z.

[36] J. J. Escobar-Chávez *et al.*, “The tape-stripping technique as a method for drug quantification in skin,” *J. Pharm. Pharm. Sci.*, vol. 11, no. 1, pp. 104–130, 2008, doi: 10.18433/J3201Z.

[37] H. Schaefer and J. C. Jamoulle, “Skin Pharmacokinetics,” *Int. J. Dermatol.*, vol. 27, no. 6, pp. 351–359, Jul. 1988, doi: 10.1111/J.1365-4362.1988.TB02374.X.

[38] T. Moolakkadath *et al.*, “Fisetin loaded binary ethosomes for management of skin cancer by dermal application on UV exposed mice,” *Int. J. Pharm.*, vol. 560, no. January, pp. 78–91, 2019, doi: 10.1016/j.ijpharm.2019.01.067.

[39] M. A. S. Abourehab *et al.*, “Sesame Oil-Based Nanostructured Lipid Carriers of Nicergoline, Intranasal Delivery System for Brain Targeting of Synergistic Cerebrovascular Protection,” *Pharmaceutics*, vol. 13, no. 4, Apr. 2021, doi: 10.3390/PHARMACEUTICS13040581.

[40] A. Correia, C. P. Costa, V. Silva, R. Silva, J. M. S. Lobo, and A. C. Silva, “Pessaries containing nanostructured lipid carriers (NLC) for prolonged vaginal delivery of progesterone,” *Eur. J. Pharm. Sci.*, vol. 153, no. May, p. 105475, 2020, doi: 10.1016/j.ejps.2020.105475.

[41] H. Tian, Z. Lu, D. Li, and J. Hu, “Preparation and characterization of citral-loaded solid lipid nanoparticles,” *Food Chem.*, vol. 248, no. November, pp. 78–85, 2018, doi: 10.1016/j.foodchem.2017.11.091.

[42] Z. Rahman, A. S. Zidan, and M. A. Khan, “Non-destructive methods of characterization of risperidone solid lipid nanoparticles,” *Eur. J. Pharm. Biopharm.*, vol. 76, no. 1, pp. 127–137, 2010, doi: 10.1016/j.ejpb.2010.05.003.

[43] G. K. Jain *et al.*, “Nano-progesterone: An improvised therapeutic approach,” *J. Pharm. Negat. Results*, vol. 13, pp. 1315–1320, Nov. 2022, doi: 10.47750/PNR.2022.13.S09.157.

[44] Ameeduzzafar *et al.*, “BBD-Based Development of Itraconazole Loaded Nanostructured Lipid Carrier for Topical Delivery: In Vitro Evaluation and Antimicrobial Assessment,” *J. Pharm. Innov. 2020 161*, vol. 16, no. 1, pp. 85–98, Jan. 2020, doi: 10.1007/S12247-019-09420-5.

[45] A. T. Alex, A. Joseph, G. Shavi, J. V. Rao, and N. Udupa, “Development and evaluation of carboplatin-loaded PCL nanoparticles for intranasal delivery,” *Drug Deliv.*, vol. 23, no. 7, pp. 2144–2153, 2016, doi: 10.3109/10717544.2014.948643.

[46] Q. Zhang, S. Li, L. He, and X. Feng, “A brief review of polysialic acid-based drug delivery systems,” *Int. J. Biol. Macromol.*, vol. 230, p. 123151, Mar. 2023, doi: 10.1016/j.ijbiomac.2023.123151.

[47] J.-S. Lan *et al.*, “Tumor-specific carrier-free nanodrugs with GSH depletion and enhanced ROS generation for endogenous synergistic anti-tumor by a chemotherapy-photodynamic therapy,” *Chem. Eng. J.*, vol. 407, p. 127212, Mar. 2021, doi: 10.1016/j.cej.2020.127212.

[48] S. Liu *et al.*, “The emerging molecular mechanism of m6A modulators in tumorigenesis and cancer progression,” *Biomed. Pharmacother.*, vol. 127, p. 110098, Jul. 2020, doi: 10.1016/j.biopha.2020.110098.

[49] W. Zeng *et al.*, “Hyaluronic acid-coated niosomes facilitate tacrolimus ocular delivery: Mucoadhesion, precorneal retention, aqueous humor pharmacokinetics, and transcorneal permeability,” *Colloids Surfaces B Biointerfaces*, vol. 141, pp. 28–35, May 2016, doi: 10.1016/j.colsurfb.2016.01.014.

[50] A. Sharma, A. P. Singh, and S. L. Harikumar, “Development and optimization of nanoemulsion based gel for enhanced transdermal delivery of nitrendipine using box-behnken statistical design,” *Drug Dev. Ind. Pharm.*, vol. 46, no. 2, pp. 329–342, Feb. 2020, doi: 10.1080/03639045.2020.1721527.

[51] J. Sharma, D. Agrawal, A. K. Sharma, M. Khandelwal, and S. Aman, “New Topical Drug Delivery System Pharmaceutical Organogel: A Review,” *Asian J. Pharm. Res. Dev.*, vol. 10, no. 1, pp. 75–78, Feb. 2022, doi: 10.22270/AJPRD.V10I1.1088.

[52] A. Gull, S. Ahmed, F. J. Ahmad, U. Nagaich, and A. Chandra, “Hydrogel thickened microemulsion; a local cargo for the co- delivery of cinnamaldehyde and berberine to treat acne vulgaris,” *J. Drug Deliv. Sci. Technol.*, vol. 58, p. 101835, Aug. 2020, doi: 10.1016/J.JDDST.2020.101835.

[53] B. G. Sharma *et al.*, “Development and characterization of budesonide pressurized metered dose inhaler using gamma scintigraphy,” *Indian J. Nucl. Med.*, 2010.

[54] N. Khan, Ameeduzzafar, K. Khanna, A. Bhatnagar, F. J. Ahmad, and A. Ali, “Chitosan coated PLGA nanoparticles amplify the ocular hypotensive effect of forskolin: Statistical design, characterization and in vivo studies,” *Int. J. Biol. Macromol.*, vol. 116, no. 2017, pp. 648–663, 2018, doi: 10.1016/j.ijbiomac.2018.04.122.

[55] S. T. Prajapati, C. G. Patel, and C. N. Patel, “Formulation and Evaluation of Transdermal Patch of Repaglinide,” *ISRN Pharm.*, 2011, doi: 10.5402/2011/651909.

[56] K. Khanna *et al.*, “Intranasal solid lipid nanoparticles for management of pain: A full factorial design approach, characterization & Gamma Scintigraphy,” *Chem. Phys. Lipids*, vol. 236, p. 105060, May 2021, doi: 10.1016/j.chemphyslip.2021.105060.

[57] D. Modi *et al.*, “Formulation and development of tacrolimus-gellan gum nanoformulation for treatment of dry eye disease,” *Colloids Surfaces B Biointerfaces*, vol. 211, p. 112255, Mar. 2022, doi: 10.1016/J.COLSURFB.2021.112255.

[58] A. Batista-Duharte *et al.*, “The Hen’s Egg Test on Chorioallantoic Membrane: An Alternative Assay for the Assessment of the Irritating Effect of Vaccine Adjuvants,” *Int. J. Toxicol.*, vol. 35, no. 6, pp. 627–633, 2016, doi: 10.1177/1091581816672187.

[59] “HET-CAM test | NIOM.” https://niom.no/het-cam-test/ (accessed Mar. 08, 2022).

[60] C. A. Aventurado, J. B. Billones, R. D. Vasquez, and A. L. Castillo, “In Ovo and In Silico Evaluation of the Anti-Angiogenic Potential of Syringin,” 2020, doi: 10.2147/DDDT.S271952.

[61] A. Nikhat, N. Hasan, Z. Iqbal, P. Kesharwani, and S. Talegaonkar, “Enhanced transdermal delivery of lutein via nanoethosomal gel: Formulation optimization, in-vitro evaluation, and in-vivo assessment,” *J. Drug Deliv. Sci. Technol.*, p. 103447, May 2022, doi: 10.1016/J.JDDST.2022.103447.

[62] I. W. Achkar *et al.*, “Metabolic signatures of tumor responses to doxorubicin

elucidated by metabolic profiling in ovo," *Metabolites*, vol. 10, no. 7, pp. 1–23, 2020, doi: 10.3390/metabo10070268.

[63] K. R. Liedtke *et al.*, "Gas plasma-conditioned ringer's lactate enhances the cytotoxic activity of cisplatin and gemcitabine in pancreatic cancer in vitro and in ovo," *Cancers (Basel).*, vol. 12, no. 1, pp. 1–19, 2020, doi: 10.3390/cancers12010123.

[64] J. Sharma and P. K. Goyal, "Chemoprevention of chemical-induced skin cancer by Panax ginsenroot extract," *J. Ginseng Res.*, vol. 39, no. 3, pp. 265–273, 2015, doi: 10.1016/j.jgr.2015.01.005.

[65] B. Iqbal, J. Ali, M. Ganguli, S. Mishra, and S. Baboota, "Silymarin-loaded nanostructured lipid carrier gel for the treatment of skin cancer," *Nanomedicine*, vol. 14, no. 9, pp. 1077–1093, 2019, doi: 10.2217/nnm-2018-0235.

[66] S. Sharma and S. Sultana, "Modulatory effect of soy isoflavones on biochemical alterations mediated by TPA in mouse skin model," *Food Chem. Toxicol.*, vol. 42, no. 10, pp. 1669–1675, Oct. 2004, doi: 10.1016/j.fct.2004.06.003.

[67] R. Pangeni, S. Sharma, G. Mustafa, J. Ali, and S. Baboota, "Vitamin e loaded resveratrol nanoemulsion for brain targeting for the treatment of Parkinson's disease by reducing oxidative stress," *Nanotechnology*, vol. 25, no. 48, Dec. 2014, doi: 10.1088/0957-4484/25/48/485102.

[68] S. M. Danish *et al.*, "Intranasal Cerium Oxide Nanoparticles Ameliorate Cognitive Function in Rats with Alzheimer’s via Anti-Oxidative Pathway," *Pharm. 2022, Vol. 14, Page 756*, vol. 14, no. 4, p. 756, Mar. 2022, doi: 10.3390/PHARMACEUTICS14040756.

[69] M. Z. Ahmed *et al.*, "Nano Matrix Soft Confectionary for Oral Supplementation of Vitamin D: Stability and Sensory Analysis," *Gels 2022, Vol. 8, Page 250*, vol. 8, no. 5, p. 250, Apr. 2022, doi: 10.3390/GELS8050250.

[70] M. K. Iqubal, A. Iqubal, H. Anjum, M. M. Gupta, J. Ali, and S. Baboota, "Determination of in vivo virtue of dermal targeted combinatorial lipid nanocolloidal based formulation of 5-fluorouracil and resveratrol against skin cancer," *Int. J. Pharm.*, vol. 610, p. 121179, 2021, doi: 10.1016/j.ijpharm.2021.121179.

[71] M. Imran, M. K. Iqubal, S. Ahmad, J. Ali, and S. Baboota, "Stability-indicating high-performance thin-layer chromatographic method for the simultaneous determination of quercetin and resveratrol in the lipid-based nanoformulation," *J. Planar Chromatogr. - Mod. TLC*, vol. 32, no. 5, pp. 393–400, Oct. 2019, doi: 10.1556/1006.2019.32.5.7.

[72] A. Sartaj *et al.*, "Ribociclib Nanostructured Lipid Carrier Aimed for Breast Cancer:

Formulation Optimization, Attenuating In Vitro Specification, and In Vivo Scrutinization," *Biomed Res. Int.*, vol. 2022, 2022, doi: 10.1155/2022/6009309.

[73] S. Bhattacharya, "Central Composite Design for Response Surface Methodology and Its Application in Pharmacy," *Response Surf. Methodol. Eng. Sci.*, Jan. 2021, doi: 10.5772/INTECHOPEN.95835.

[74] C. M. Chung, S. J. Wee, H. Lim, S. H. Cho, and J. W. Lee, "Skin malignancy initially misdiagnosed as a benign epidermal cyst," *Arch. Craniofacial Surg.*, vol. 21, no. 2, p. 123, 2020, doi: 10.7181/ACFS.2019.00752.

[75] L. D. de Moura *et al.*, "Docetaxel and lidocaine co-loaded (Nlc-in-hydrogel) hybrid system designed for the treatment of melanoma," *Pharmaceutics*, vol. 13, no. 10, 2021, doi: 10.3390/pharmaceutics13101552.

[76] A. Qadir *et al.*, "Nanostructured lipidic carriers for dual drug delivery in the management of psoriasis: Systematic optimization, dermatokinetic and preclinical evaluation," *J. Drug Deliv. Sci. Technol.*, 2020, doi: 10.1016/j.jddst.2020.101775.

[77] M. C. Cristiano, A. Mancuso, E. Giuliano, D. Cosco, D. Paolino, and M. Fresta, "EtoGel for Intra-Articular Drug Delivery : A New Challenge for Joint Diseases Treatment," 2021.

[78] S. Paliwal *et al.*, "Flurbiprofen loaded ethosomes - transdermal delivery of anti-inflammatory effect in rat model," *Lipids Heal. Dis. 2019 181*, vol. 18, no. 1, pp. 1–15, Jun. 2019, doi: 10.1186/S12944-019-1064-X.

[79] N. Hasan *et al.*, "Formulation and development of novel lipid-based combinatorial advanced nanoformulation for effective treatment of non-melanoma skin cancer," *Int. J. Pharm.*, p. 122580, Jan. 2023, doi: 10.1016/J.IJPHARM.2022.122580.

[80] C. J. Gordon, "The mouse thermoregulatory system: Its impact on translating biomedical data to humans," *Physiology and Behavior*, vol. 179. Elsevier Inc., pp. 55–66, Oct. 2017, doi: 10.1016/j.physbeh.2017.05.026.

[81] P. V. Pople and K. K. Singh, "Targeting tacrolimus to deeper layers of skin with improved safety for treatment of atopic dermatitis—Part II: In vivo assessment of dermatopharmacokinetics, biodistribution and efficacy," *Int. J. Pharm.*, vol. 434, no. 1–2, pp. 70–79, Sep. 2012, doi: 10.1016/j.ijpharm.2012.04.051.

[82] E. B. Kurutas, "The importance of antioxidants which play the role in cellular response against oxidative/nitrosative stress: Current state," *Nutrition Journal*, vol. 15, no. 1. BioMed Central Ltd., Jul. 25, 2016, doi: 10.1186/s12937-016-0186-5.